Statistical characterisation of seismic reflectivity patterns with applications to the Rockall Basin

RSG Project 92/2

Annual Report 2001

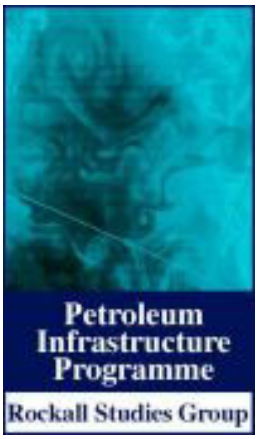

Padraic Mac Aodha

Introduction

This final annual report for RSG project 97/2 coming as it does during the write up stage of the project contains details of those sections of the project that have been fully documented to date. A brief introduction to the project outlining its scope and why it was undertaken is presented in Chapter One. This will be followed by a look at VECSTAT algorithm the project is based on and how this has been developed and improved over the course of the work. Chapter Three looks at the technical detail behind the implementation if the theory discussed in Chapter Two. Some of the applications of the algorithm will be looked at in particular the tools it provides for the statistical characterisation of deep seismic profiles. Chapter Five will examine the data used from the Rockall basin and surrounding regions and the results of VECSTAT's statistical analysis of this data.

The deeper parts of vertical incidence seismic sections are difficult to interpret, as they do not display simple reflectivity patterns. Scattering and problems with attenuation lead to an absence of clear reflections with resulting problems in developing velocity profiles all of which means that the deeper parts of seismic profiles show little interpretable geological pattern. In order to extract as much information as possible from these profiles, the VECSTAT algorithm was developed for the statistical characterisation of these reflectivity patterns. The analysis performed by the algorithm allows regions such as thinned rifted basement and unstretched continental basement complexes to be statistically compared and distinguished, using statistical parameter such as vector mean, circular variance and total energy. The algorithm handles data in a rastified or pixelated formula i.e., (x,y,flag) which makes it very versatile in the range of data formats it can work on. Industry standard SEGY, paper copies of profiles and CDVU have all been used as data sources during the course of the project.

These methods have been applied to seismic profiles in the Rockall Basin region using the BIRPS WIRELINE and WESTLINE deep seismic data sets, and a network of commercial lines (Fig. 1). The commercial lines, mainly shot as exploratory surveys in the 1970s and all available in the public domain, show varying degrees of penetration of the basement. Most of the data is from within the basin itself, mainly in the Northern Irish sector. Data for the western margin is limited to four lines, which traverse the entire basin

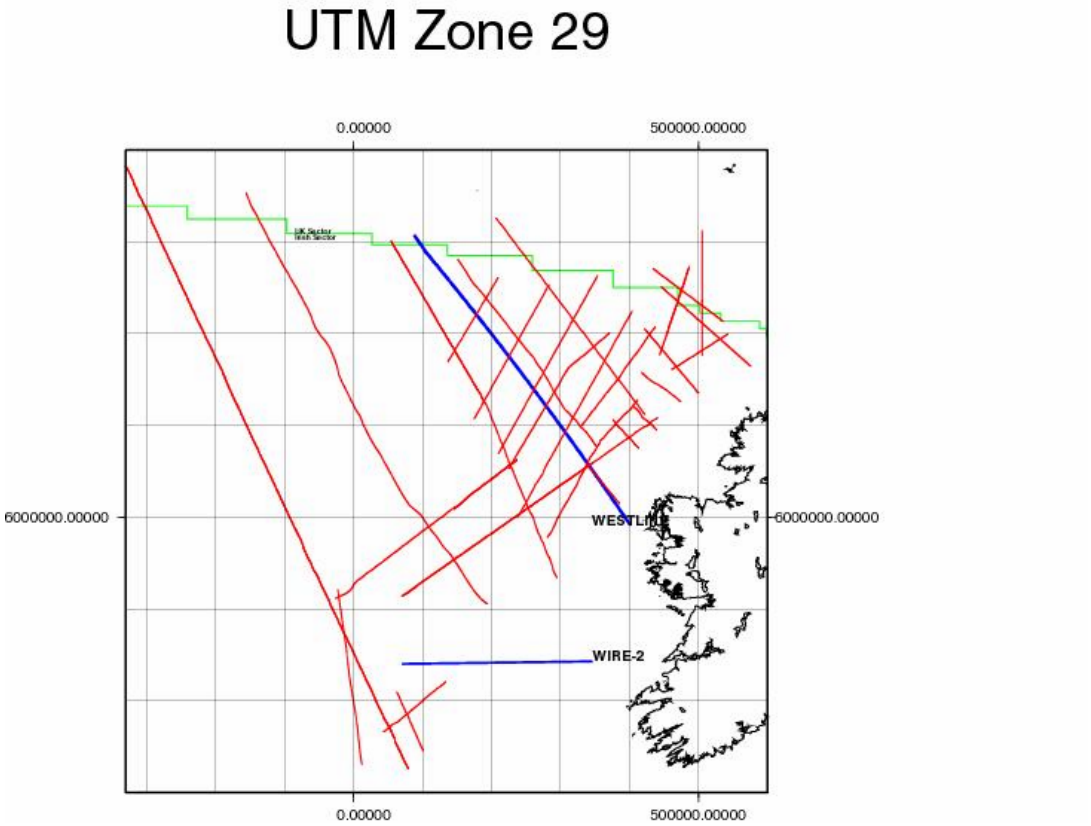

Figure 1.1: *location map showing the lines used in the Rockall Basin area, commercial lines are shown in red BIRPS lines in blue and the boundary between the UK and Irish sectors is shown in green.*

1.1 Geological Setting

1.1.1 Location

The Rockall Basin is a large sedimentary basin lying of the coast of Ireland and Scotland, delineated by the bathymetric expression of the Rockall Trough, which it was referred to as in the literature before the official PAD Nomenclature (Naylor *et al*. 1999). It is 1200 km along its axis and up to 300 km wide. Water depths increase rapidly from 200-300m on surrounding highs to over 2000m on the basin floor and approach 3000m in the southwest of the basin.

It is bounded by a series of basement highs and tertiary compression features. To the Northeast it is separated from the Faeroe Shetland Basin by the Wyville Thompson Ridge. Its eastern margin is made up of the Erris High, Slyne High and Porcupine High which separate it from landward basins of the same names. On the margins of these highs and on the Porcupine High in particular sit perched basins namely Colm, Fursa, Macdara, Padraig, Brona (North and South) and Cillian as you move form north to south. To the south and southwest the boundary between the basin and the Porcupine Abyssal Plain is marked by the Charlie Gibbs Fracture Zone, a large scale

transform fault. To the west the basin is bounded by the Rockall Bank, which separates the basin from the shallower Hatton Basin on the Rockall Plateau. Again the margin contains a series of perched basins, Ciaran Conal and Ronan (Naylor *et al.* 1999).
This study will concentrate on the section of the basin and surrounding margins and highs contained within the Irish designated area i.e., the southern boundary to 56-57^{o}N, delineated in green on Figure 1.1.

1.1.2 Tectonic History

The Atlantic margin formed as Pangea split apart in a series of discrete rifting phases starting in the Early Permian. Sea floor spreading started in the Central Atlantic bay the Middle Jurassic (165 Ma) and spread northwards with oceanic crust present between Newfoundland and Iberia by 110 Ma. The Bay of Biscay and the Labrador Sea opened by 83 Ma and Greenland was separated from the Rockall Plateau by 53 Ma. Pre-existing lineaments played a pivotal role in defining the orientations of rift axis during the Mesozoic and Cenozoic, proto North Atlantic for example took place along a zone of NE-SW Caledonian terrane boundaries that traversed both sides of the present Atlantic during Devonian times (Knott *et al*. 1993). There follows an examination of the tectonic events that affected the region from the Devonian to the present.

1.1.2.1 Devonian - Late Jurassic

At the end of the Caledonian orogeny (Early to Middle Devonian) the Iapetus and mid-European oceans had closed and the plates of Laurentia, Baltica, Avalonia, and Armorica had joined to form the Old Red Continent assembly (Ziegler 1990). The Caledonian mountain belt underwent orogenic collapse resulting the formation of localised mollasse basins, e.g., Orcadian in Scotland. Small pull-apart basins such as the Clare Basin were formed when left lateral motion was induced on the Great Glen Fault by collision of Gondwanaland and Laurasia. This Hercynian orogeny culminated in Stephanian time with Gondwanaland moving North into Laurasia resulting in the inversion of Late Devonian and Carboniferous basins on the UK Continental Shelf (Ziegler 1990).
Plate reconstruction work by Knott *et al*. (1993) allows for some end-Carboniferous to Early Permian stretching (β=1.5) in the proto North Atlantic but not as much as the 300 km suggested by Russell (1973, 1976), and Haszeldine (1984). Rifting continued on the proto North Atlantic rift and various other localities on the Eurasian foreland on a series of N-S trending fault systems, into the Early Permian. By Zechstein time in the Late Permian thermal subsidence had replaced rifting resulting in a marine transgression from the with deposition marine source rocks. Knott *et al*. (1993) suggest significant stretching in the proto North Atlantic during the Early Triassic (β=1.8) orthogonal to documented Triassic faults in the North Sea. This stretching was replaced by Late Triassic (Smith *et al*. 1993). Some rifting (β=1.1) the northern moving south to the central North Sea during Oxfordian to Kimmeridgian (Rattey and Hayward 1993). During the late Jurassic anoxic conditions prevailed in the North Sea due to restricted circulation through the narrow Goban spur, these conditions are also thought to have prevailed in proto North Atlantic pull-apart basins. This continued until the early Valanginian when circulation and oxic conditions were restored (Knott *et al*. 1993).

1.1.2.2 Cretaceous

The Early Cretaceous saw the cessation of rifting in the North Sea but with continued rifting on the proto-North Atlantic. It is the mid-Aptian rift episode related to the onset of rifting in the Bay of Biscay and the Labrador Sea which was the main contributor to the present day configuration of the Rockall Basin (Roberts 1978, Makris *et al*. 1991).

During the rifting significant footwall uplift occurred along the proto-North Atlantic margins which it is expected would result in erosional unconformities, redeposition of shallow marine clastics and footwall-derived debris flow deposits. Such sediments have been found in the Faeroe-Shetland Basin (Knott *et al*. 1993). By late Cretaceous the opening of the Rockall Basin was finished leaving the Rockall plate and the failed Rockall Basin attached to the European plate The rifting now jumped to the other side of the Rockall Plateau as it started to move with the European plate away from Greenland. Knott *et al*. (1993) put a data of 83 Ma on this movement based on the age of Anomaly 34 which passes south of the basin. The late Cretaceous collision between Iberia and Eurasia resulted in an approximately NE-SW compressional stress been transmitted to the Eurasian foreland with associated structural inversion.

1.1.2.3 Tertiary-Present

The Atlantic rifting taking palace to the northwest of the Rockall Plateau was effected by a major hotspot which resulted in a circular dome of uplift 2000 km across centred under Greenland. The Rockall Basin and Faeroe-Shetland Basin were uplifted by at least 1.5 km (Joppen and White 1990). The doming associated with the hot spot resulted in the reactivation of NW trending basement features which served to compartmentalise the basins in the region (Knott *et al.* 1993). The opening of the NE arm of the Atlantic between Greenland and Europe, was initiated at 53 Ma and by 50 Ma oceanic crust separated the Rockall Plate and Greenland.

Compression between the spreading ridge and the Alpine Mountain Belt resulting in margin uplift could be responsible for the Early Eocene unconformity. Tectonic uplift related to the Pyrenean event has been suggested as a cause for the mid-Oligocene regional unconformity (Knott *et al*. 1993). Following this period to the early Miocene the Rockall Basin saw the deposition of shallow marine clastics progressively onlap the base Oligocene unconformity.

1.1.2.4 Pre-Cretaceous Rifting?

The Rockall Basin is one of a system of basins that were formed during Mesozoic attempts to open the North Atlantic (Musgrove and Mitchner 1996). The general scheme of this large scale tectonic event is broadly agreed upon but the exact timing and nature of the opening of the various basins involved is still a matter of some debate. This is particularly true of the Rockall basin, normal incidence reflection seismic data from the region are typically of poor quality owing to the effect of shallow tertiary sills which mask the nature of and hence the age of deeper strata in the basin. Coupled with this is a lack of well control, very few wells have been drilled in the area and only three the basin itself, none of these has been in the Irish sector.

There is much discussion in the literature as to the occurrence and the extent of pre-Cretaceous rifting in the basin and hence the age of the sedimentary layers contained within. This has been fuelled to no small part by the importance of Mesozoic sediments in hydrocarbon exploration on the Atlantic Margin.

Arguments against pre-Cretaceous rifting are based on the relatively thin nature of the sedimentary succession (5-6 km) compared with 10-15 km surrounding basins. There is also the absence of a pre-Cretaceous sediment in what wells in the basin sampled that deep. Wells from surrounding basins however such as well 12/13-1 located in the Erris Basin encountered a Permo-Triassic section overlain by a thin Jurassic section. These are unconformably overlain by an Early Cretaceous section. Similar evidence is available in the Slyne and Porcupine basins (Croker and Shannon 1987). Well 164/25-1 encountered a Triassic section with syn-rift stratal geometry. These wells indicate rifting in the region of a Triassic and Late Jurassic age. However the only well that has penetrated Mesozoic sections within the Rockall Basin itself, 132/15-1, encountering a section of Early Cretaceous age, interpreted as syn-rift in age from seismic sections, lying directly on crystalline basement (Musgrove and Mitchner 1996).

Musgrove and Mitchner (1996) put forward two rift trends for the Atlantic margin based on the history of basins on both sides of the Atlantic. Triassic/Jurassic rift systems are documented in the Jeanne D'Arc, Porcupine, Slyne, Erris, Minch and Faeroe-Shetland basins. The Porcupine, Slyne, Erris and Hebredean Basins show little or no evidence of Cretaceous rifting imposed on their earlier Triassic/Jurassic rifts. In the Jeanne D'Arc Basin the Triassic/Jurassic rifting trends NE toward the Porcupine Basin while the Cretaceous rift system trends NW to the Orphan Basin. This Cretaceous rift system is considered to have continued from Orphan to the Rockall Basin and the Faeroe-Shetland Basin. Their analysis of seismic reflection data, well data and rift trends found no evidence of pre-Cretaceous rift events but at the same time nothing to preclude them.

England and Hobbs (1997) working on data form the BIRPS WESTLINE interpreted a single rift episode and identified the syn-rift sediments as Cretaceous. They also stated that if any Jurassic sediment is present it must be very thin as expanding spread profile data indicated that Cretaceous sediments lie directly on basement velocity rocks.

Shannon *et al*. (1995) however contend that the difference in sedimentary thickness can be accounted for by sedimentary starvation during the Mesozoic with the bulk of continentally derived sediment trapped in more proximal landward basins such as Porcupine, Slyne Erris, and Donegal. Upper Palaeozoic sediments were encountered by drilling in Porcupine, (Croker and Shannon 1987), Slyne (Danier *et al*. 1999), Erris (Chapman *et al*. 1999), and Donegal and are also predicted in the Rockall Basin (Naylor *et al*. 1999). The presence of perched basins with considerable thickness of sedimentary fill analogous to that of the Slyne and Erris Basins (Corfield *et al*. 1999) suggests that similar sediments should be present in the Rockall Basin though considerably thinned by subsequent rifting.

2D modelling carried out by Nadin *et al*. (1999) concluded that using a *ß*-factor of 2.2 for Cretaceous rifting within the basin, independently estimated from plate reconstruction work, an initial water depth of 1500m and Moho depth of 20 km prior to Cretaceous rifting is required to provide a good fit. Plate reconstruction work by Cole and Peachy (1999) required a *ß*-factor of 1.6 for pre-Cretaceous rifting.

1.1.3 Structure

Despite early assertions that the crust in the basin was oceanic (Roberts *et al*. 1981; Joppen and White 1990) wide angled refraction/reflection studies such as the RAPIDS profiles (O'Reilly et. al. 1995; Hauser *et al*. 1995) have shown that thinned but unbreached continental crust extends west from Ireland beneath the Rockall Basin and Rockall Plateau to the Hatton continental margin.

The RAPIDS data show a three layer crust beneath onshore Ireland the Irish shelf and again beneath the Rockall bank has been thinned to two layers under the Rockall Basin with a sedimentary cover of 5-6 km. The RAPIDS profiles also revealed a low velocity layer below the Moho interpreted by O'Reilly *et al*. (1996) as serpentinite. The thinning of the continental crust from 30 km onshore and Rockall Bank to 5 km, with up to 8 km sediment and water overburden (O'Reilly *et al*. 1994), in the basin requires beta factors in the region β =5-6. Two theories have been put forward to explain how such severe rifting could have occurred without any evidence of crustal rupture or voluminous underplating and igneous intrusion. First is the idea that rifting was multiphase spread out from as far back as the Triassic to the middle Cretaceous, the magnitude of each discrete rifting event would be small (β=2) but the cumulative effect would be large (Walsh *et al*. 1999; Cole and Peachey 1999).

The second model requires differential stretching of the lithosphere in the region, with the lower crust stretched by a factor of 2-3 while the more brittle upper crust accommodates stretching in the region of 8-10 (Hausner *et al*. 1995). This differential stretching is results in the fusing of the middle and upper crustal layers explaining the transition from a three layer crust on the bounding highs to a two layer crust in the basin.

Three main structural trends have influenced the evolution of evolution of the Rockall Basin NE-SW, N-S and NW-SE (Corfield 1999). The first two are the most important in terms of Mesozoic basin development and define the trends of the basins bounding faults. The NW-SE lineaments are interpreted as transfer zones similar to those seen in the Faeroe Shetland Basin, motion along lineaments of this orientation has served to compartmentalise the basins.

1.1.4 Igneous Activity

Decompression melting due to rifting and the presence of the Iceland Plume have resulted in widespread and voluminous magmatism on the Northern Atlantic Margin (Hitchner *et al.* 1997). Thick igneous sills are present in large areas of the basin these are considered to be predominately Tertiary in age (Morton 1988) but Cretaceous volcanics have also been described from seamounts in the region (Shannon *et al.* 1995). Musgrove and Mitchner (1996) suggested that since sills inject at subsurface depths where the overburden pressure equals the magma pressure (Einsele 1985) and as they are seen throughout the thick Upper Cretaceous section becoming more common where the Cretaceous crustal thinning was the most extreme, some of the sills may be Cretaceous in age. The second Tertiary wave can be correlated with those in the Faeroe-Shetland Basin and are attributed to volcanism associated with the Iceland Plume. The sills typically occur on seismic sections at 2 sec TWTT below the seabed (Shannon *et al.* 1995) and act as a significant barrier the penetration of near vertical incidence seismic energy.

Two large areas are affected in the basin itself. The area surrounding the Barra Volcanic Ridge System in the south of the basin. The ridges themselves can be described as a series of curvilinear-shaped igneous bodies believed to be

predominantly Early Cretaceous in age. Where they appear on lines WI-32 and GSI Line 1 they are covered by a drape of Tertiary sediments (Naylor *et al.* 1999).

Theory

VECSTAT

VECSTAT is an image analysing algorithm, which allots values to pixels in the image derived from the spatial distribution of the surrounding filled pixels. It does this by setting up a counting circle around each point as illustrated in Figure 2.1. The size of this counting box delineates the region in which the algorithm sources data to attribute values to a particular point. A pixel can be defined as the smallest incremental point on which the image is built. For the black and white images analysed by VECSTAT a filled pixel is a black pixel (i.e., there is data present at that point) and an empty pixel is a white pixel (no data present). Three statistical values; vector mean, circular variance and total energy are attributed to the point, depending on the location, distribution and quantity of filled pixels within the counting circle.

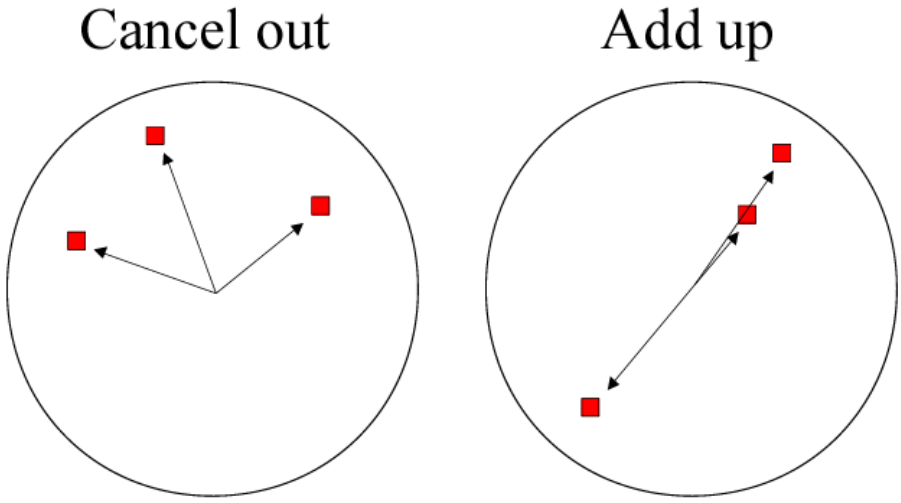

Figure 2. 1*: A counting box is set up around each point in the image, each of the filled pixels in the counting circle is then allotted a unit vector value which are summed to give a vector mean over the entire circle. Vectors which line up get added while those that are random cancel each other out.*

2.1 Vector Mean

Vector mean is calculated by allotting each filled pixel within the counting circle a unit vector quantity. The vectors for the box are then totalled. The vectors from aligned pixels add up while those which are from a random distribution of pixels cancel each other out (Figure 2.1). Thus if an alignment is present the vectors from its pixels will dominate and the point will be allotted a vector mean representative of that alignment orientation.

Unit vectors are used instead of the real vector lengths in order to avoid an disproportional influence been brought to bear by vectors for filled pixels on the edge of the counting circle. By using unit vectors the resulting orientation is more influenced by larger populations of filled pixels with a common alignment than random pixels on the edge of the circle. The use of unit vectors is also computationally much more efficient (see section 3.2.2).

Certain filters were added to the initial theory in order to improve resolution and

accuracy of the vector mean being produced. The problems which necessitated the introduction of the filters is first examined followed by a look at the filters and their effectiveness

2.1.1 Minimum Length

This filter sets a minimum length for vectors or more accurately distance between the centre of the counting circle and the filled pixel. It was introduced to counteract the distorting effect of vectors representing filled pixels close to the centre of the counting circle when bands of data wider than one pixel are been imaged. Figure 2.2 shows an example of a counting circle centred over a broad band of data which is assumed to have either all filled pixels within the band or a random distribution of pixels. The vectors in each of the four quadrants will average around the median of that quadrant as the area of the data band on either side of the median is the same. Since only the orientations are important to VECSTAT calculation of the orientation A and A^1 (A^T) will be seen as the same orientation as will B and B^1 (B^T). Therefore, the overall orientation will be the average of A^T and B^T vectors weighted for the total area of the data band in each section. While A^T has the larger area and hence will dominate the resulting orientation, B^T will non the less have and effect and will skew the resulting orientation away from the true orientation. The effect of the B^T orientation on the overall result increases linearly as the thickness of the data band increases from 1 pixel wide where total $B^T = 0$ to where the band is wider than the circle and B^T is at a maximum and equal to A^T. This situation can be improved by the introduction of the minimum length filter which has the effect of rendering the data in the centre red circle void (Fig. 2.2 right). More of the area of A^T will be removed than of B^T but the percentage of B^T which is removed is much greater than that of A^T hence the result is biased toward that of A^T or the true orientation of the data band.

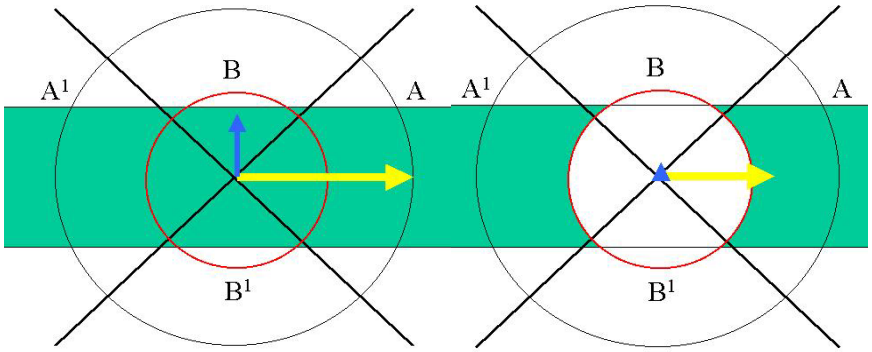

Figure 2.2 *The left diagram shows how the vectors average out in each quadrant with A^T in yellow averaging on the true orientation, but with B^T strong enough to skew the result. On the right we see the situation following the elimination of the data within the red circle by the minimum length filter both vectors are reduced but the effect on B^T is much greater.*

The Figure 2.4 below shows the results of a vector mean analysis for the image of lineaments of various orientations shown in Figure 2.3, without and with the filter. In the section analysed without the filter shown on the left very little of the true orientation of the lineaments is showing through and we just see a progressive movement of orientations around to perpendicular to the true orientation (see section 2.1.2 below). With the filter in place on the left, the situation has changed to a clear

band of true orientation data in the centre with a sharp boundary to the flanking perpendicular data on either side.

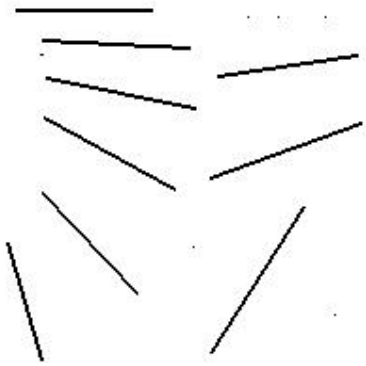

Figure 2.3 *Test panel II used as a source for the data used to test the improvements made VECSTAT to help it more clearly resolve vector mean. It consists of a series of lineaments of various orientations and some isolated filled pixels to illustrate the effect of noise in the data.*

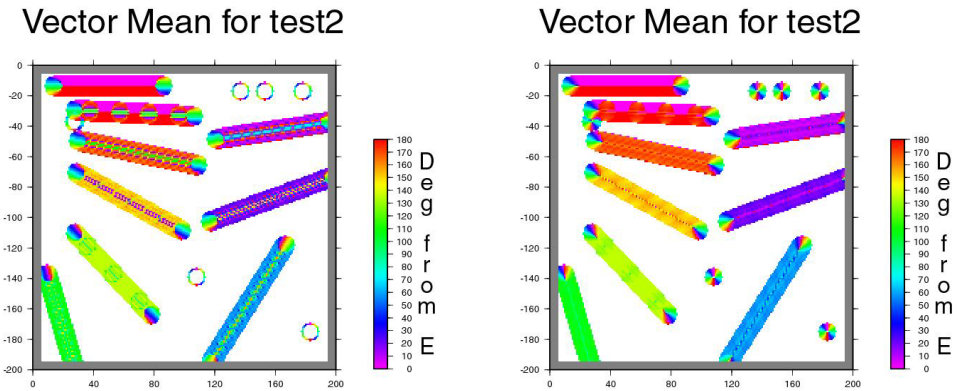

Figure 2.4 *Vector mean analysis for test panel II (Fig. 2.3) without (left) and with (right) the minimum length filter the orientations are measured as dips into the lower hemisphere from the horizontal.*

2.1.2 Minimum Filled pixels

This filter which requires a certain number of filled pixels to be present in a counting circle before data from that counting circle is accepted was introduced to prevent VECSTAT from creating data perpendicular to the true orientation in areas bordering data bands. To best explain the problems which arise, a theoretical example will be examined in detail. Three stages of the movement of the counting circle across a horizontal band of data will be examined.

2.1.2.1 Counting Circle on Middle of Data Band

This situation has already been explained in Section 2.1.1 and Figure 2.2 above. As

explained above it gives an accurate representation of the true orientation of the data band.

2.1.2.2 Counting Circle Centre Within Data Band

Figure 2.5 illustrates this situation where the centre of the counting circle is still in the band but it is no longer centred on it. The area of B^T has shrunk and will continue to do so until it reaches a minimum when the centre of the counting circle is centred on the edge of the band. However B has under gone a proportionally greater increase in size and therefore the total area of data within B^T has increased. The area encompassed by it is still symmetrical about its median and so the vectors will average to the median. The area of A and A^1 will decrease as the centre of the counting circle moves off the centre of the band and toward the edge. More importantly however the area encompassed by A or A^1 is no longer symmetrical about the orientation of the data band and hence the vector mean for either A or A^1 separately will be skewed from the true orientation of the band. When added the combined area will however still average to the true orientation. Like in the first instant, more overall area is removed from A^T by the minimum length vector but when percentages of overall area are considered B^T again fares worse and therefore the filter is still advantageous. Still the reduction in the area of A^T and of the effective of that area combined with the increased area of B^T mean that once you move off the centre of the band the vector mean starts to progressively move away from the true orientation.

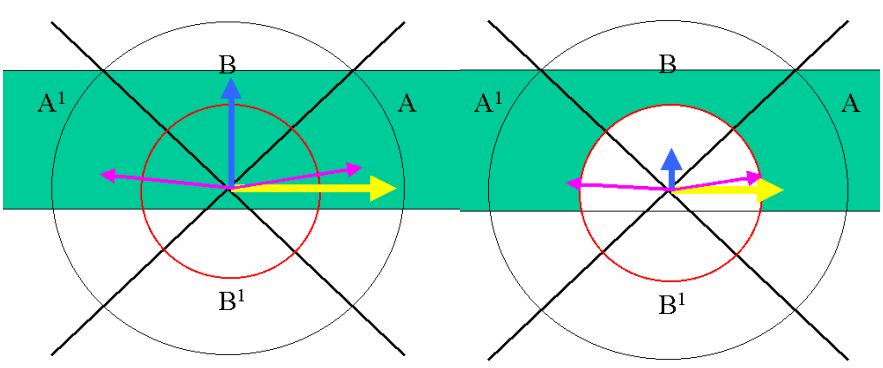

Figure 2.5 *Shows the situation when the centre of the counting circle is within the data band but not on its midpoint, without (left) and with (right) minimum length filter.*

2.1.2.3 Counting Circle Centre on Either Side of the Band

In this case illustrated in Figure 2.6, while there is no data in B^1 the area of B^T is greater than A^T. A and A^1 will still average around the true orientation but it is more than over powered by B^T. The vector mean for this situation will rapidly move to perpendicular to the true orientation as the centre of the counting circle moves away from the edge of the band.

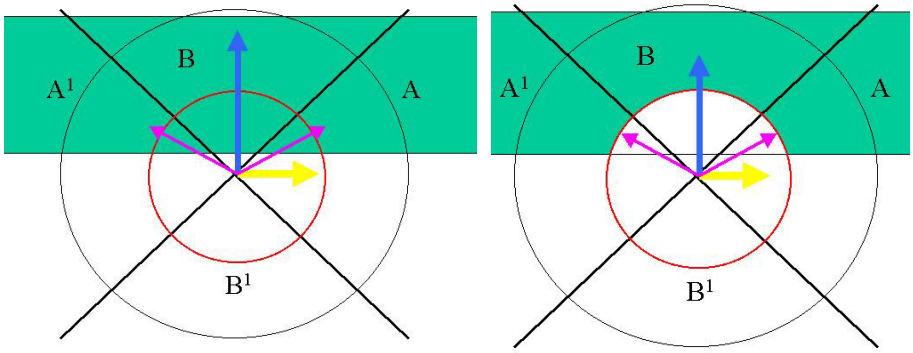

Figure 2.6 *Shows the situation when the centre of the counting circle is outside the band without (left) and with (right) the minimum length filter.*

In summary as the midpoint of the counting circle moves down across the data band you get a series of data shown in Figure 2.7. The central band shown in green where the vector mean will reflect the true orientation results from the first situation described above. Flanking this shown in orange is a band of skewed orientation resulting from the second situation described above. Finally, this is in turn flanked by the result of situation three, bands of orientation perpendicular to the true orientation. The problem is that while the width of the central three bands will only be the width of the band of data, the outer bands will be the width of the radius of the counting circle. However in order to image the band of data properly the diameter of counting circle (also equal to the combined with of the outer perpendicular) so there will always be more results of perpendicular to the true orientation than reflecting it.

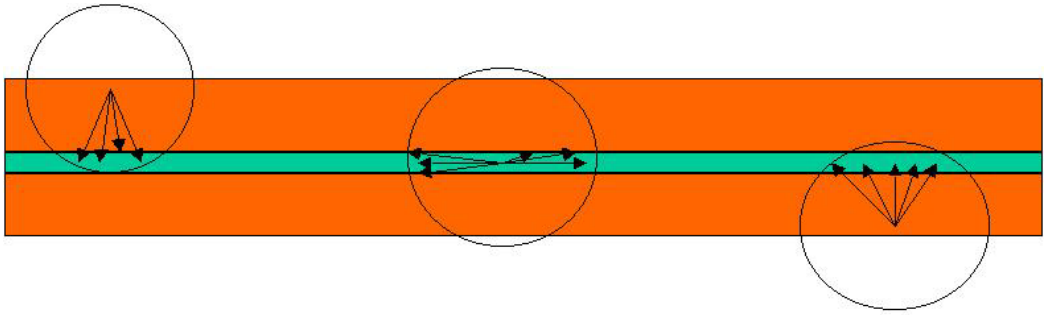

Figure 2.7 *True orientations are only produced while the centre of the counting circle is within the data band shown in green otherwise perpendicular vector means are produced in the bands shown in orange.*

The minimum length filter can increase the accuracy of the skewed band by reducing the effect of the B^T area but it has no effect on the areas of perpendicular data. This problem leads to the introduction of a second filter which set a minimum quantity of data which must be present in the counting circle before its orientation is accepted as valid. The maximum number of filled pixels will be present when the centre of the counting circle is over the centre of the band. Therefore, by increasing the severity of

the filter the bands on either side of the filter can be reduced until only the true orientation section is left (Fig. 2.8).

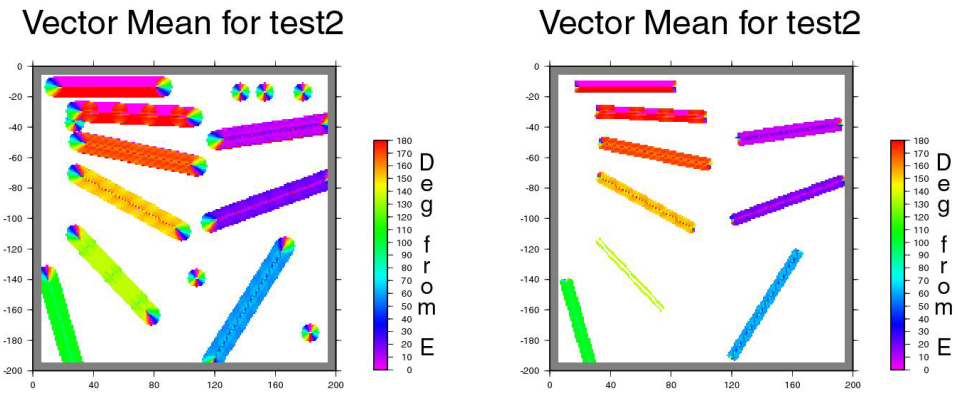

Figure 2.8 *The effect of the minimum filled pixels filter is illustrated by the reduction in the width of the perpendicular vector mean bands in the right plot compared to the left where the filter is not applied. Also note the spheres showing the full range of vector mean have disappeared.*

This filter also eliminates the problem of single, or small groups of random data common in noisy seismic sections creating a multiplied amount of noise in the resulting data. The multiplier being a factor of the size of the counting circle. When the counting circle incurs a single filled pixel or a small group of bunched pixels it will attribute an orientation for every point whose counting circle intersects solely with the group or single filled pixel. Figure 2.9 illustrates how a circle of varying orientations will be created around a single filled pixel as it moves over the area.

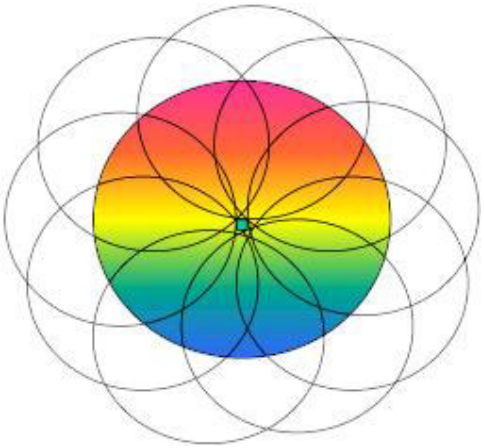

Figure 2.9 *A circle with a complete range of vector orientations is created around a single pixel shown in the centre in green, in the absence of a minimum filled pixels filter.*

2.1.3 Conflict Between Filters

As shown above the minimum number of pixel's filter is effective in eliminating both the perpendicular data and noise created by random points. A problem arises however when the two filters are used together. The minimum number of pixel's filter works as

a maximum amount of data or filled pixels is encountered when the counting circle is centred over the centre of the band, when the minimum length filter is informed. However the maximum number of filled pixels is no longer encountered when both centres line up but when the band lies on either side of the removed centre circle (Fig 2.10). When this happens it is the real orientations which are first to go as the severity of the minimum number of pixels filter is increased as they are now based on a smaller area and hence less pixels.

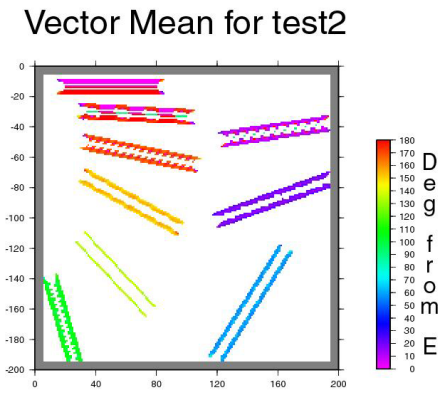

Figure 2.10 *The application of both filters results in the elimination of the true vector means before the perpendicular vector means.*

Both filters therefore cannot be used together as they conspire to irradiate all real vector means and leave only perpendicular vector means.

2.1.4 Counting Ellipses

For reasons discussed in the previous section it is not possible to use both the minimum length and the minimum filled pixel filters effectively on the same data set. The effects of the minimum length are however still desirable if not necessary so an alternative method for reducing the effect of B^T was sought. The most effective method found was to reduce the counting area in the B^T direction by changing the shape of the counting circle to an ellipse. The counting ellipse is moved across the image incrementally in the same manner as the counting circle but with the added step that for each pixel the ellipse is rotated through 180^o. The use of ellipses not only reduces B^T in wider data bands where it is a problem but also eliminates the effect of stray pixels near lineaments in noisy seismic data. By using ellipses the algorithm is effectively biased toward focussed lineaments as it no longer has to consider stray filled pixels which are present in the area of a lineament but not actually part of it (Fig. 2.11).

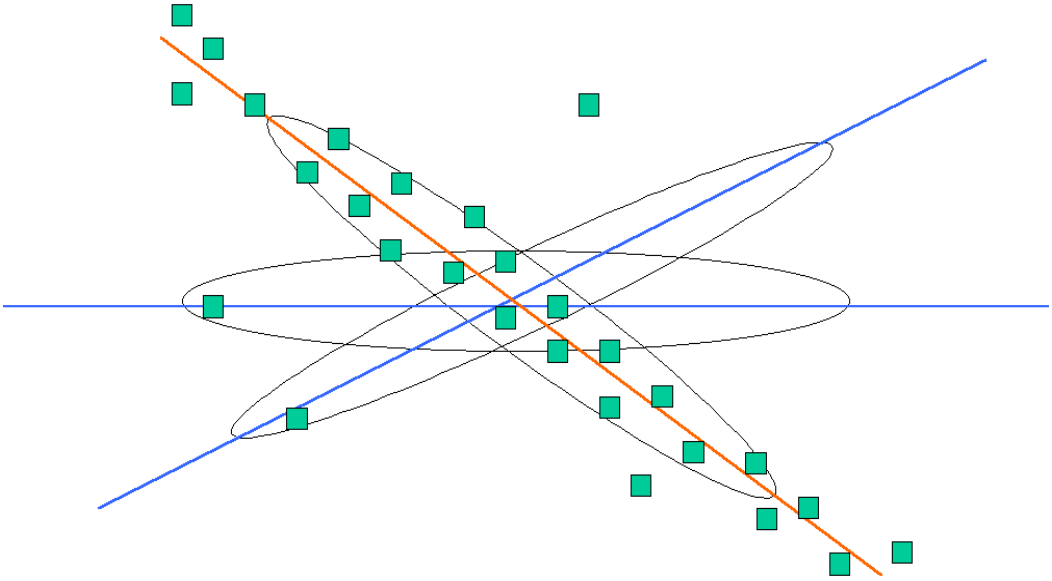

Figure 2.11 *Shows the uses of ellipses instead of counting boxes. The filled pixels are assessed in an ellipse of every orientation and the orientation which best fits the lineation (shown in red) is taken as the vector mean.*

As the algorithm now chooses its preferred orientation on the basis of which ellipse contains the most filled pixels and as no area from the centre of the ellipse needs to be removed from the calculations to reduce the effect of B^T the minimum length vector is no longer required as it is effectively built in. As the true orientation will always have the maximum number of filled pixels the minimum filled pixels filter will not remove true orientation vector means till last.
The effectiveness of the ellipse format in reducing B^T is illustrated below in Figure 2.12. On the left we see how B^T has been greatly reduced with strong bands of true vector mean data flanked by the perpendicular data. On the right the minimum filled pixel filter has been applied to leave just the true vector means. This results in what is an accurate evaluation of the vector means or the orientations of the lineaments shown in the original image (Fig. 2.3) within the constraints of the colour range used.
This is the form of the algorithm which will be used to evaluate vector mean.

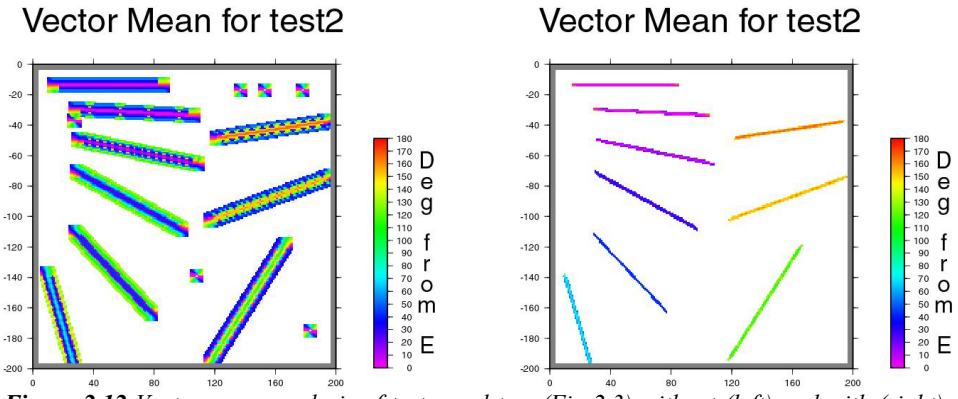

Figure 2.12 *Vector mean analysis of test panel two (Fig 2.3) without (left) and with (right) minimum filled pixel filtering.*

2.1.5 Remaining Problems

There are however problems which can arise with VECSTAT. If the diameter of the counting ellipse is less than the width of the band the algorithm becomes confused by the glut of filled pixels and is not able to distinguish the alignment of the pixels as each orientation will contain approximately the same amount of filled pixels. It is totally surrounded and from its limited perspective, it is surrounded by a random distribution of pixels (Fig. 2.13). This will result in a random scatter of vectors in the centre of broad bands if the size of the counting ellipse is not increased.

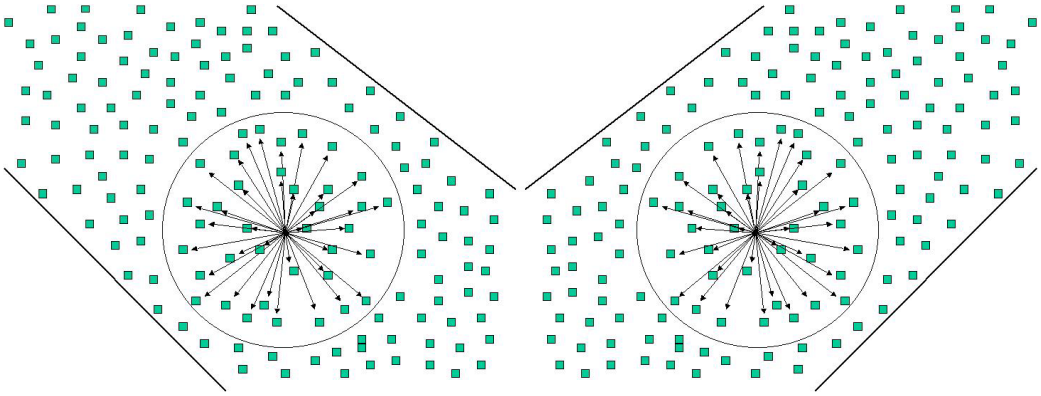

Figure 2.13 *The two circles enclose the area that will be examined by the counting ellipse for any one point. Each of the orientations the ellipse is put through will contain approximately the same amount of filled pixels. When the band of data is wider than the long axis of the ellipse, the diameter of the circles, the algorithm is not able to distinguish between the two orientations above.*

The second case is when the pixels between parallel lines, such as the parallel reflections present at the top sedimentary sections of most seismic sections, are been analysed. In this case if the size of the counting circle is greater than the with, gap between the lines, then for points within the gaps the vectors in the counting circle will be dominated by the lines above and below (Fig. 2.14). The effect of this is to give a band of points with trends up 90^{o} to the trend of the parallel lines. This problem can be countered by using smaller counting circles but this is not often desirable as it leads to its own problems such as the counting circle fitting inside larger bands of data as described in the previous paragraph (see Section 3.2.1.1). A carefully chosen minimum filled pixels filter is sufficient to avoid this problem in most cases as unless the parallel lineaments are broad compared with the average data bands the sections shown will contain less filled pixels than an ellipse on a lineament.

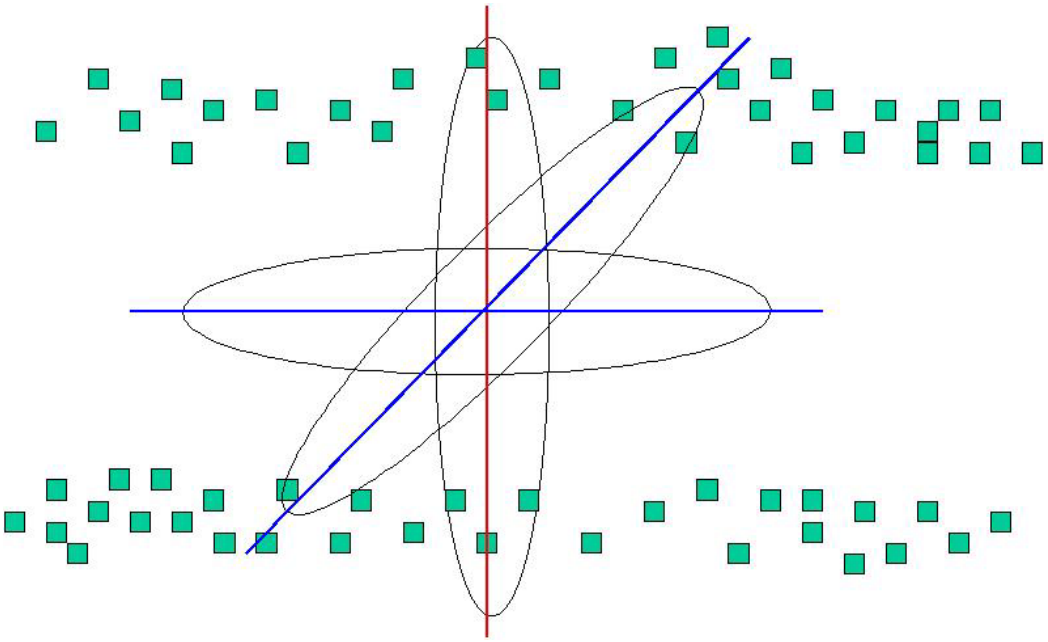

***Figure 2.14**: When the counting circle is between two parallel lines it is dominated by the pixels at either side and the point ends up with a orientation perpendicular to the parallel lines.*

2.2 Circular Variance

Circular Variance is essentially a measure of the degree of scatter of the pixels within the counting circle. Counting circles are used as per the original theory (Fig. 2.1) as using ellipses, a different circular variance would result for each of the 180 increments analysed and each result would only be valid for that ellipse. The aim is however to get a measure of scatter in the entire area encompassed by 180 orientations of the counting ellipses so the counting circle is much more efficient. It is calculated as its inverse by dividing the length of the summed vectors by the total number of vectors present. The more aligned the pixels in the counting circle are the longer the value of the summed vector will be and hence the higher the value of the inverse of the circular variance will be (Equ. 2.1).

$$= 1/\text{Circular Variance} = \text{Total length} / \text{No. of Vectors} \qquad \text{Equ. 2.1}$$

Circular variance suffers from the same problems as vector mean when dealing with broad bands. If the counting circle is in the centre of a broad band as illustrated in Figure 2.13 the total number of vectors will be high but the summed length of those vectors will be low as they cancel each other out. This results in a high circular variance at the centre of lineations.

Circular variance can also be used as a filter by blanking all pixels with a large circular variance i.e., a random scatter of vectors within the counting circle. One problem with using circular variance as a filter is that it will remove the centre of broad reflections.

2.3 Total energy

Total energy is a measure of the amount of data in the image analysed. Total energy for any point is simply the number of filled pixels present in the counting circle for that point. It acts as a good quality control to check that the results are representative of what we put and that we are not creating or losing data at any stage. As with circular variance total energy is calculated using a counting circle to evaluate the total number of filled pixels in the area encompassed by all 180 orientations. Total energy can also be used as a filter to clean up random noise by blanking any pixels whose total energy is below a certain value from the image before the vector analysis is carried out. This can if used carefully remove background noise from around reflections but not within. The smaller the counting box used too the more extensive the areas that can be filtered but the less subtle the cut off point can be and visa versa.

Method

In this chapter the application of the theory examined in the last chapter will be discussed addressing the following topics. Methods used for data extraction from all formats encountered. The workings of the VECSTAT suite of software together with the mathematical formula used in the calculation of the statistical parameters measured. Finally the methods used to graphically portray the results.

3.1 Data Extraction

Some of the more effective methods of extracting the data are detailed below including those used to extract the data on Rockall. The list is by no means exhaustive but does cover at least one method for the variety of data formats to which VECSTAT has been applied. VECSTAT analysis data in a pixelated format i.e., x co-ordinate, y co-ordinate, flag (the flag is usually 1 for filled pixels and 0 for empty but setting a cut-off point from a range of values is possible (see Section 3.2.1.3).

3.1.1 Scanned images

Extracting the data to (x,y,flag) when dealing with paper only copy data it is simply a matter of scanning the data and converting it to a monochrome XPM graphics format. Most modern graphics packages support the XPM format however where it is not possible tiff files of windows X bitmap format serve as good intermediary formats. JPEG and GIFF formats tend to result in loss of resolution and blurring of edges and are therefore not recommended. Once the data is in XPM format VECSTAT's ancillary scripts can convert the data to (x,y,flag).

The XPM format is a text based graphical storage format (Fig.3.1) (Le Hors 2001). Its files consist of header information giving details as to the size of the image and what colours are attributed to each symbol used to represent the image. For a monochrome XPM image there should be only two symbols present (black usually represented by a point "." and white represented by a space " ") if there are more than two symbols used it is not a monochrome file and should be converted to one before continuing. Below the header information the data is laid out in lines with the symbol for each pixel (point in the image) in the location it appears in the image. The start of the lines are denoted by an inverted comma and the end by and inverted comma and a comma. The VECSTAT script (Appendix X) uses sed commands to remove the header and the inverted commas and commas in the lines of data. Sed commands are then used to convert the black pixel symbols to "1" and the white to "0" spaces between the "1"'s and "0"'s are also inserted. An awk script was then used to convert attribute Cartesian co-ordinates to the pixels the spaces used as field separators. The resulting output is data in the (x,y,flag) format.

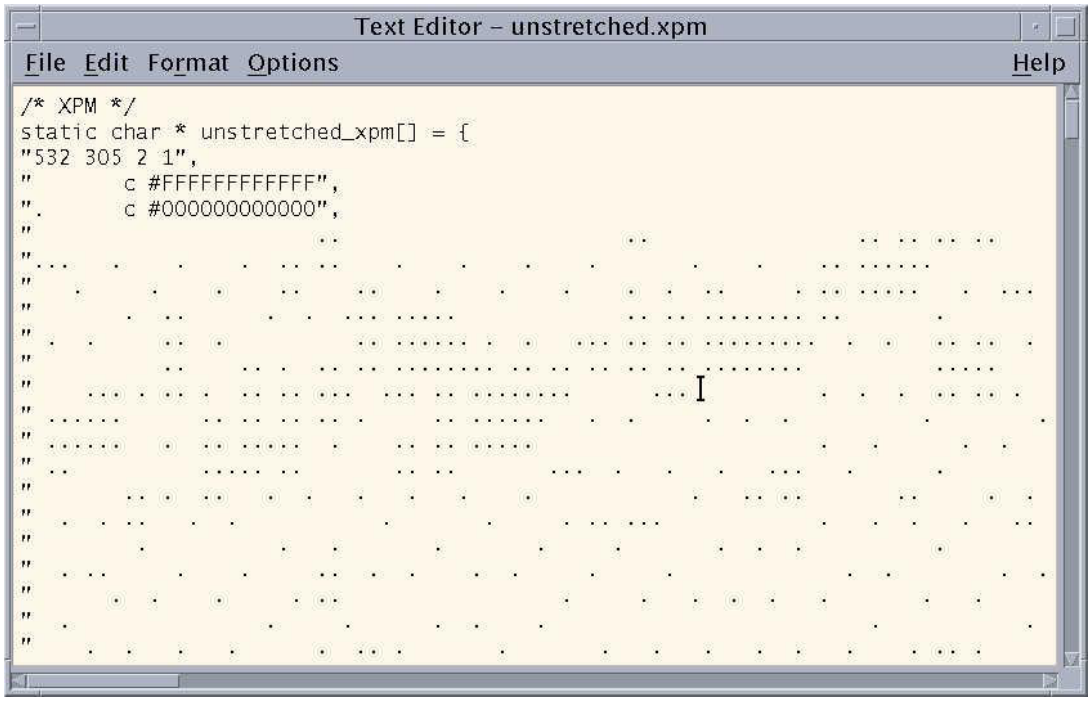

Figure 3. 1 *Screen snapshot of an XPM file showing the file header defining the two symbols used "." and " ", and other information such as the size of the image. Below this is the image mapped out in symbols.*

3.1.2 SEGY Files

While one of the advantages of the method is the ability to analyse data which is only available in paper copy use of the data in its original SEGY format which is far more efficient. Three main options for converting data from SEGY to (x,y,flag) were explored during this work and they are outlined below.

3.1.2.1 Rough Printing Module

The first method uses the rough draft printing module which is part of the Claritas software package. This module rasterises a variable area form of the seismic trace and saves it to a text file to be fed to the printer. The module makes use of a threshold parameter which controls how much data is sent to the rough plot. It sets the amplitude above which the printer will print a variable area representation of the nature of the trace. Only positive amplitudes are used. The resulting text file consists of ones and zeros laid out in the position of the pixels they represent. As this is the same as one of the intermediate stages of the conversion from XPM it can be converted directly to (x,y,flag). However as it is designed to send the data to a spool printer it outputs the data in portrait form and so the data undergoes a simple transform to rearrange the data in landscape. This method has the advantage that the Threshold parameter can be used to filter a certain amount of noise out of the data before VECSTAT analysis it. It is also quick and easy to perform once an optimum threshold value has been established. It does not however allow full control over the scale on the plots produced and this becomes a problem in comparisons between data from different sources (see Section 3.1.2.4).

3.1.2.2 Advanced Printing Module

The second method again involves using one of the printing modules of the Claritas seismic processing package. This time it is the detailed printing module used to produce good quality prints of seismic lines. While the module used in the above method and how it works may be unique to Claritas a printing module such as this will be available with all seismic processing software. In this case the section of line to be analysed is outputted sent as a Variable Area plot to an rtl file. Variable area plots are used as the horizontal lines in wiggle trace plots are not part of a valid VECSTAT dataset. The rtl format is the result of a printing language developed by Hewlard Packard (1997) and must be converted to XPM format before VECSTAT can take over. In this study the conversion was carried out using the Xrtl module on Claritas to convert to a tiff file and from there to XPM using Solaria's image viewer. As with the method a transform is applied to switch from landscape to portrait. This printing module has the added advantage of been able to set the vertical horizontal scales which as mentioned above is important when dealing with data from different sources. It does not however have a threshold option and all data is sent to the plot. The extraction is also much more unwieldy and lengthy to perform.

3.1.2.3 Freeware and Shareware Options

There are a number of freely available software packages which facilitate the viewing of seismic profiles without the need for commercial processing packages. Both the US Geological Survey (Goldman 1999) and the GMT (GMT 2001) mapping package offer tools for converting SEGY files to (x,y,z) files so they can be viewed without the need for seismic processing software. These files can be converted for use with VECSTAT.

3.1.2.1 Scale

As VECSTAT'S vector mean analysis is based on the spatial arrangement of the filled pixels surrounding the pixel been analysed, its results are susceptible to anything which may distort that spatial arrangement. A change in the ratio of the x-axis scale to the y-axis scale will result in a change in the vector mean produced. When dealing with non-seismic data or even when analysing a single seismic line this is not a problem. When a large scale study is involved however differences in scales between profiles and in particular between profiles from different surveys do arise. In order to safely compare results from a range of profiles and surveys, the scales must be homogenised. To do this efficiently, it must be possible to set the horizontal and vertical scale to counteract the fact that the numerous surveys from which lines have been taken for this study have used different receiver group spacing and hence different CDP spacing.

3.2 VECSTAT

The operation of VECSTAT package can be broken down into four categories, input

files, the analysis code, the output files and the plotting scripts, each of which will be examined in turn.

3.2.1 Input Files

Two input files are used the actual data file and the parameter file both standard ASCII files. The data file (with a .dat file extension) consists of the data in simple x, y, flag format in three columns separated by spaces. (details of how this was arrived at see previous section). The co-ordinates must be presented in descending order for each row of pixels moving from left to right i.e., starting at the top left and moving down to the bottom right. If the data is not presented to VECSTAT in this order the orientation of the vector mean will not be correct.

The parameter file (with a .inp file extension) (Figure 3.2) consists of a series of parameters or variables, which are fed to the VECSTAT executable. By having these parameters in a small separate file instead of contained within the VECSTAT code it is easy to vary them without the need to recompile the code. The first four parameters are simple file system directions which tells VECSTAT where to find the files necessary to run data file, GMT files, etc.

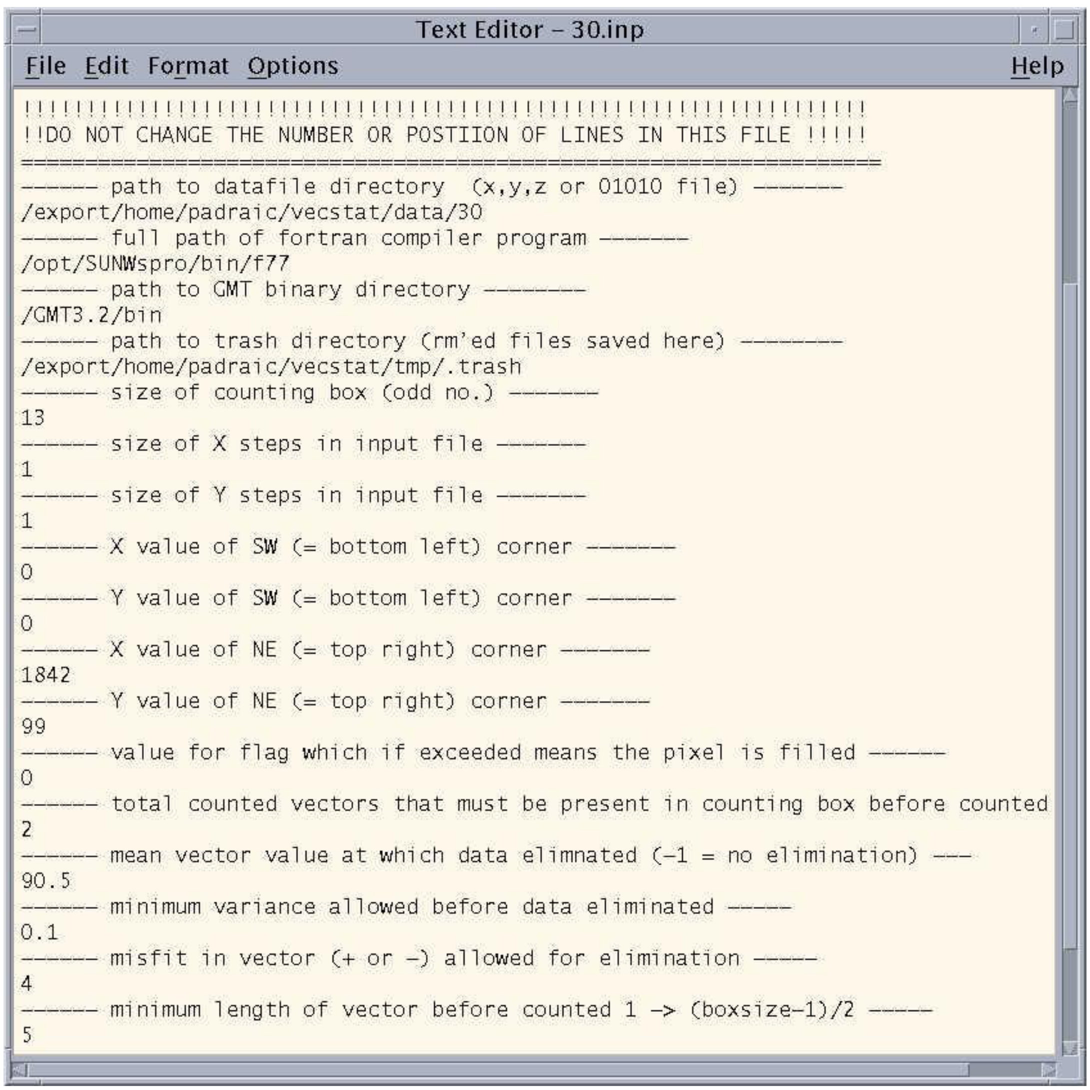

Text Editor – 30.inp

File Edit Format Options Help

```
!!!!!!!!!!!!!!!!!!!!!!!!!!!!!!!!!!!!!!!!!!!!!!!!!!!!!!!!!!!!!!!!!
!!DO NOT CHANGE THE NUMBER OR POSTIION OF LINES IN THIS FILE !!!!!
===================================================================
------ path to datafile directory  (x,y,z or 01010 file) -------
/export/home/padraic/vecstat/data/30
------ full path of fortran compiler program -------
/opt/SUNWspro/bin/f77
------ path to GMT binary directory --------
/GMT3.2/bin
------ path to trash directory (rm'ed files saved here) --------
/export/home/padraic/vecstat/tmp/.trash
------ size of counting box (odd no.) -------
13
------ size of X steps in input file -------
1
------ size of Y steps in input file -------
1
------ X value of SW (= bottom left) corner -------
0
------ Y value of SW (= bottom left) corner -------
0
------ X value of NE (= top right) corner -------
1842
------ Y value of NE (= top right) corner -------
99
------ value for flag which if exceeded means the pixel is filled ------
0
------ total counted vectors that must be present in counting box before counted
2
------ mean vector value at which data elimnated (-1 = no elimination) ---
90.5
------ minimum variance allowed before data eliminated -----
0.1
------ misfit in vector (+ or -) allowed for elimination -----
4
------ minimum length of vector before counted 1 -> (boxsize-1)/2 -----
5
```

Figure 3.2 *Sample .inp file used to feed parameters to VECSTAT, the significance of each vector is explained below.*

3.2.1.1 Counting Circle

The next parameter is the size of the counting circle to be used. This is the radius of the long axis of the counting ellipse for the calculation of vector mean and of the counting circle for the calculation of circular variance and total energy It is important that this parameter is set correctly in order to optimise the statistical analysis performed by VECSTAT. If the value is set too low the sample size of the counting circle is too low to grasp the overall trend and vector value attributed to that pixel may be overly influenced by random noise. Small counting circles will also become overwhelmed by broad bands of reflected energy (see Section 2.1.5) often found in deep seismic profiles. At the other end of the scale the higher the scale is set the more resolution is lost as data further and further away from the point starts to affect its vector value. While shallow parallel reflections are not easily dealt with by this method and require careful minimum filled pixels filtering it is worth noting that, to deal with shallow parallel reflections properly the counting circle must be small enough to fit between the reflections. Generally values between 9 and 19 were used in the scope of this study. Figure 3.4 below illustrates the effect of increasing the size of the counting ellipse from 10 on the left to 18 on the right for vector mean analysis of test panel I (Fig 3.3). While both results show accurate vector mean results there are some notable differences. The area enclosed in the circle on the bottom centre shows a sharp kink in the lineation present this is picked up by the smaller counting ellipse size but is too small to be imaged properly by the larger one. Conversely in the highlighted circle on the upper right hand side the larger counting ellipse images the continuation of the lineation present across the gap in the data but the smaller counting ellipse does not succeed in making the connection.

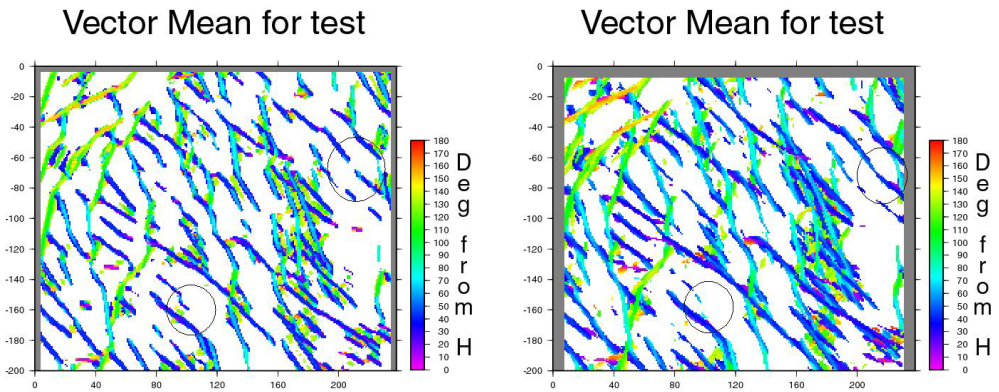

Figure 3.4 *Vector mean for test panel one analysed with counting ellipse sizes 10 on the left and 18 on the right.*

3.2.1.2 Ellipse Ratio

This parameter sets the degree of ellipticity of the counting ellipse used to evaluate

vector mean. The value entered is the ratio of the long axis to the short axis. In general this ratio is kept low especially when the corresponding counting circle parameter or long axis radius is low. In general the ellipse must be wide enough to incorporate sufficient filled pixels to derive an accurate orientation but narrow enough to keep the effect of pixels not involved in the general lineament been imaged from interfering with the overall orientation. Figure 3.5 illustrates the effect of increasing the ratio from top left to bottom right, it is clear to see that the resolution and accuracy of the vector means derived improves dramatically as the ellipse is narrowed from 3:1 to 10:1, this is the optimum level for this counting ellipse size (15) and further narrowing to 15:1 does not improve resolution but results in minor loss of true vector mean data (see Fig 2.3 for source data).

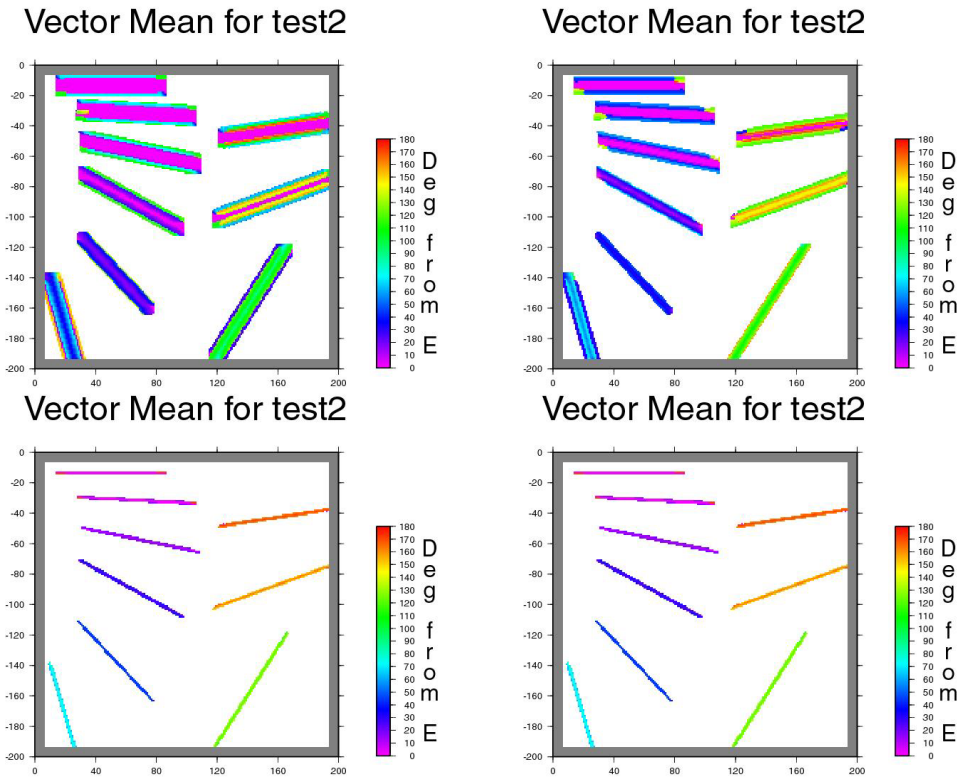

Figure 3.5 *Vector mean for test panel two with the following ratios of the long axis to the short axis , 3:1 top left, 5:1 top right, 10:1 bottom left, and 15:1 bottom right.*

3.2.1.3 Grid Co-ordinates

The next two parameters set the size if the increments of the co-ordinates in the data file, usually set to 1. The following four parameters are the co-ordinates of the bottom left and bottom right of the data set. When the whole data set is been used they are just used by VECSTAT to calculate what size of an array it is going to be handling. By setting these values appropriately, a subset of the data can be analysed. This is useful when trying to assess the best processing parameters (counting circle, filled value, total counted vectors, variance, vector length) to use on a large data set.

3.2.1.3 Flag Value

This is the value for the flag for each point above which the pixel is taken as been filled. Normally the data is converted to a format where the flag is either one or zero and this parameter is set to zero but it is possible to have a range of flag values and in these cases this parameter sets the level above which the flag is taken as a filled pixel.

3.2.1.4 Minimum Filled Pixels

This filter prevents plotting of data for counting circles/ellipses that contain less than a certain number of filled pixels. It was introduced to VECSTAT cut out perpendicular vector means and to prevent the analysis from creating circles around lone or marginal filled pixels and hence producing noise in the data. See section 2.1.4 for a full description.

3.2.1.5 Elimination Value

This parameter is used by VECSTATS vector elimination tool. VECSTAT allows for the elimination of data of a certain orientation. This data can then be analysed separately or the remaining data exported for further analysis (see section 4.3). Value is entered in degrees between 0 and 180 with 90^{o} representing the horizontal.

3.2.1.6 Minimum Variance

This is a filter for the data being extracted, it sets an upper limit on the circular variance permissible at a point. If the circular variance is exceeded, the point will not be extracted. It must be a value between zero and one as this is the range for circular variance data.

3.2.1.7 Misfit in Vector

This is the degree of latitude either side of the Elimination Value defined above which is accepted. It is used to extract vectors in a band of orientations and not just a single orientation. Even when trying to extract a vector of specified orientation it is best to allow some degree of latitude to allow for the resolution of the analysis

3.2.1.8 Minimum Length

This parameter is designed to prevent the pixels near the centre of the counting circle masking the overall trend. It is necessary due to the fact that each vector is given a unit value. For a full explanation see Section 2.1.1.

3.2.2 Algorithm

The theory behind the VECSTAT algorithm has already been outlined in the previous chapter but in this section the calculations undertaken by the algorithm will be examined. The VECSTAT programme reads in the data from the .dat file. Since counting circles are used for calculation of circular variance and total energy and a

rotating ellipse is used to calculate vector mean, the algorithm performs two analyses at each point. The calculation of circular variance and total energy using a counting circle will be dealt with first.
For each point in the data, the algorithm calculates which filled pixels lie within its counting circle as defined in the parameter file (see Section 3.2.1.1). This is tested by checking if the pythagorean distance d between the point been analysed and the filled pixel in question is less than the radius set.

$$d = [(x_1-x_2)^2 + (y_1-y_2)^2]^{1/2}$$

where (x_1,y_1) are the co-ordinates of the centre of the counting ellipse and (x_2,y_2) are the co-ordinates of the pixel.
For each pixel that lies within range sine and cosine of the angle are calculated.

$$\sin Ø = Y/d$$

$$\cos Ø = X/d$$

where Ø is the angle made with the horizontal, X is the x-axis component of the vector and Y is the y-axis component.

The total number of valid vectors in the counting circle is noted as this will give the total energy for the counting circle. When all the vectors present in the counting circle have been calculated they are summed to give the resultant vector shown in red in Figure 3.6.

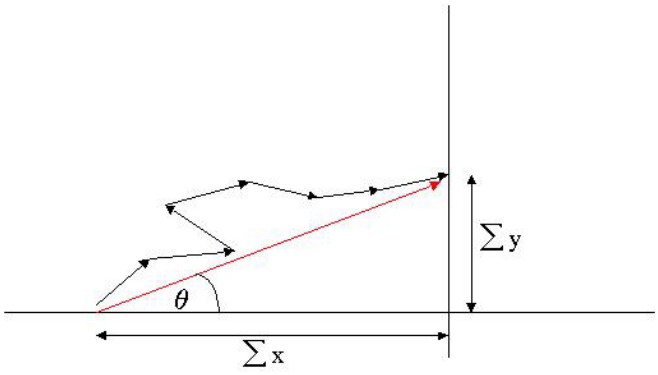

Figure 3.6 *The resultant vector shown in red is comprised of Σx the sum of the x-axis component of each of the unit vectors and Σy the sum of the y-axis component of each of the unit vectors.*

Once the orientation of the individual vectors have been calculated the distance values for them are discarded and they are then treated as unit vectors. This is because it is the position of the filled pixel with respect to the centre of the counting circle that is important, not its distance for the centre.
The x-axis and y-axis component for any of the individual vectors is

$$X = d(\cos \text{Ø})$$

$$Y = d(\sin \text{Ø})$$

From Figure 3.6 we can see that for the resultant vector the x-axis component is given by the sum of the x-axis components for each of the individual vectors

$$\Sigma x = d(\cos \text{Ø}^1) + d(\cos \text{Ø}^2) + d(\cos \text{Ø}^3) + d(\cos \text{Ø}^4) + ...$$

but as we are dealing with unit vectors d = 1 so

$$\Sigma x = \cos \text{Ø}^1 + \cos \text{Ø}^2 + \cos \text{Ø}^3 + \cos \text{Ø}^4 + ...$$

$$\Sigma x = \Sigma \cos \text{Ø}$$

similarly

$$\Sigma y = \Sigma \sin \text{Ø}$$

These two values are calculated by the algorithm on a continual basis as each new vector is orientation is assigned.
Circular variance is given by

$$Cvar = 1 - D/\text{No. of vectors}$$

Where D is the length of the resultant vector given by

$$D = [(\Sigma x)^2 + (\Sigma y)^2]^{1/2}$$

The No. of vectors present has already been counted for the total energy statistic. Both these values are then attributed to the co-ordinates, been analysed and outputted to var.xyz in the case of circular variance and num.xyz in the case of total energy. These and the other output files created will be looked at in more detail in Section 3.2.3.

To calculate vector mean an ellipse is used instead of a counting circle (see Section 2.1.4). The orientation of the pixel and its distance d from the centre of the counting circle are calculated.

$$d = [(x_1 - x_2)^2 + (y_1 - y_2)^2]^{1/2}$$

where (x_1,y_1) are the co-ordinates of the centre of the counting ellipse and (x_2,y_2) are the co-ordinates of the pixel. The orientation of the pixel is given by

$$\sin \text{Ø} = Y/d$$

$$\text{Ø} = \sin^{-1}(Y/d)$$

The distance from the pixel to the centre of the circle is compared with the radius of the ellipse in the direction Ø which is given by.

$x_e = a (\sin Ø)$
$y_e = b (\cos Ø)$

where (x_e,y_e) are the co-ordinates of the ellipse in at the angle Ø.
The data set is then rotated incrementally through 180 degrees which has the same effect as rotating the ellipse only simpler. The orientation of the ellipse (i.e., the amount of rotation of the data set) which gives the maximum of filled pixels is taken to be the best fit for vector mean. This vector mean is then attributed to the point for which the counting circle was set up and outputted to the vec.xyz with those co-ordinates.
The orientation of the resultant vector for the ellipse which had an minimum associated circular variance could also be taken as vector mean. However this produced no improvement in accuracy and was abandoned as it is computationally more intensive.

3.2.3 Output Files

VECSTAT produces a series of output files, data files which contain the results of the statistical analysis, filter files which contain the data of certain orientation which has been filtered out and information files which contain details about the analysis performed and the original data. The function of each of these files will now be examined.
The data files which are vec.xyz, var.xyz and eng.xyz contain the results of the vector mean, circular variance and total energy analysis, respectively. They are text files containing x co-ordinate y co-ordinate and the relevant value for each point analysed.
The filter files consist of cleanfill.out consisting of the data of the prescribed orientation that has been removed by VECSTAT. Its counterpart cleandat.out contains the remaining data after the extraction of the prescribed orientation. As with the data files they are text files with data in the (x,y.flag) format ready for further analysis.
The information files range.txt and dat.txt contain information about the size of the data set and the parameters used in the analysis. In the case of range.xyz the dimensions of the data set are written in a format that can be used by the plotting scripts to decide on the size of plot required.

3.3 Plotting

The analysed data was graphically represented using the GMT suit of mapping tools GMT (2001). Before the data could be plotted it was adjusted to account for the discrepancy between the conflicting ways VCESTAT and GMT look at the data. GMT because to was originally developed as a mapping package expects data to be ordered from the bottom left to the top right while as mentioned in the previous section VECSTAT takes data ordered from top right to the bottom left. In order it overcome this an Awk script was applied to the data making the y values negative thus flipping the data.
VECSTAT produces vector orientations in the range $0\text{-}180^o$ however as it is customary to represent dips with the horizontal as the origin instead of the vertical orientations in the Northwest sector were converted to the Southeast sector so they

could be colour coded as degrees above or below the horizontal.
With these adjustments made the results were gridded using the xzy2grd tool and the image plotted using the grdimage tool, scales and headers were added using the psscale tool. Further information on theses tool and GMT software is available from the GMT web site.

Applications

4.1 Statistical characterisation of Crustal Types

Different crustal types display different reflectivity patterns depending on their geological makeup. Using the VECSTAT algorithm it is possible to statistically characterise the reflectivity patterns from various crustal types. The expected reflectivity patterns from different crustal settings will be outlined below including a type section example for each setting.

4.1.1 Unstretched Crust

This crustal type can be described as unrifted old crystalline basement such as that found on the continental margins on either side of the Rockall Basin. The homogenous nature of this crust type makes it noisy but acoustically transparent in terms of the emergence of any clear reflections. Figure 4.1, 4.2, 4.3 show the vector mean total energy and circular variance plots respectively for four sections of unstretched to very mildly stretched basement. The panel on the top left, labelled AIR_0-1940 shows a section of line AIR78-88 from the Irish shelf to the east of the Slyne Basin. The panel on the top right labelled WI-01A_2-4, shows a section of line WI-01A where it crosses the northwestern corner of the Porcupine High. The panel to the bottom left images another section of WI-01A further to the southwest but still on the Porcupine High. The panel to the bottom left contains the northwestern end of WI-22 where it images the Cliona High.

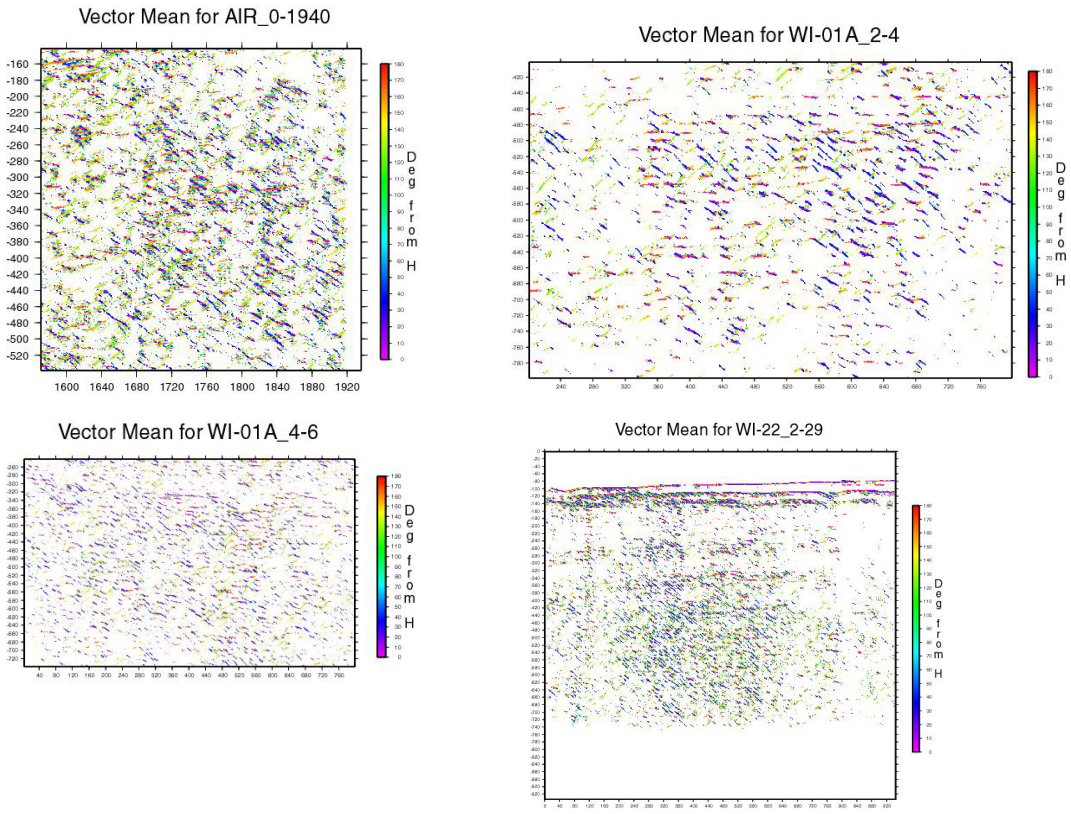

Figure 4.1: *Vector mean plots for sections of AIR-78-88 (top left), WI-01A (top right), WI-01A (bottom left), WI-22 (bottom right) (see text for location), the vector means have been colour coded as per the*

scale bars with orientations increasing clockwise from the horizontal.

The vector mean plots show the random nature of the reflected energy in this crustal type, with a full range of orientations dispersed evenly through all four sections. The exception being the top of WI-22_2-29 where the sediment water interface and the interface between the thin layer of sediment and the underlying crystalline basement provide a series of coherent reflections. Another marked contrast between the other data present and these coherent reflections is the lack of lateral continuity in the reflected energy from the crystalline basement. It is necessary to point out that the apparent trend dipping to the bottom right of the images is due to the fact that dark blue which represents that orientation is preferentially picked out by the eye and is not real. If the colour scheme was rotated 90^{o} the apparent trend would be to the top right.

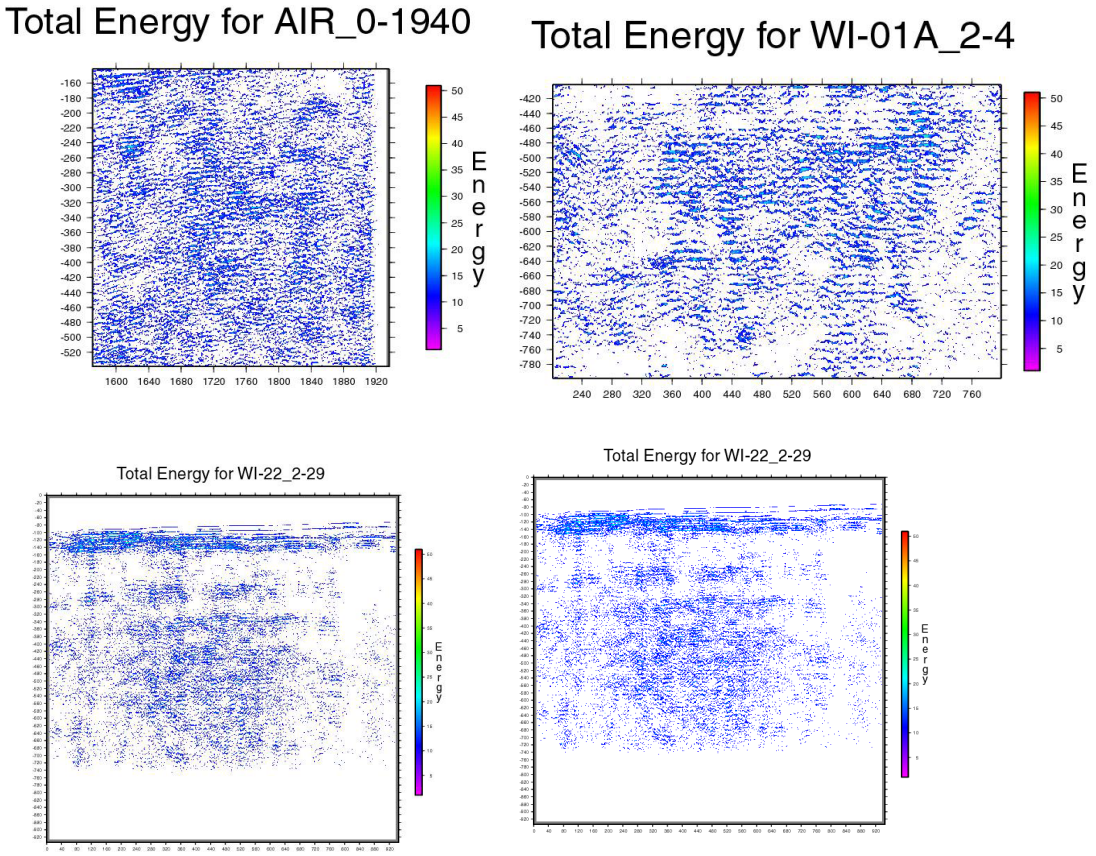

Figure 4.2: *Total energy plots for sections of AIR-78-88 (top left), WI-01A (top right), WI-01A (bottom left), WI-22 (bottom right) (see text for location), the colours show total energy present per counting circle.*

The total energy plots show reasonably high total energy returns in the 10-20 filled pixels per counting circle (counting circle radius 17). The plots illustrate the dispersion of the energy returned with the exception of the concentration at top of WI-22_2-29 where the coherent reflection horizons are present.

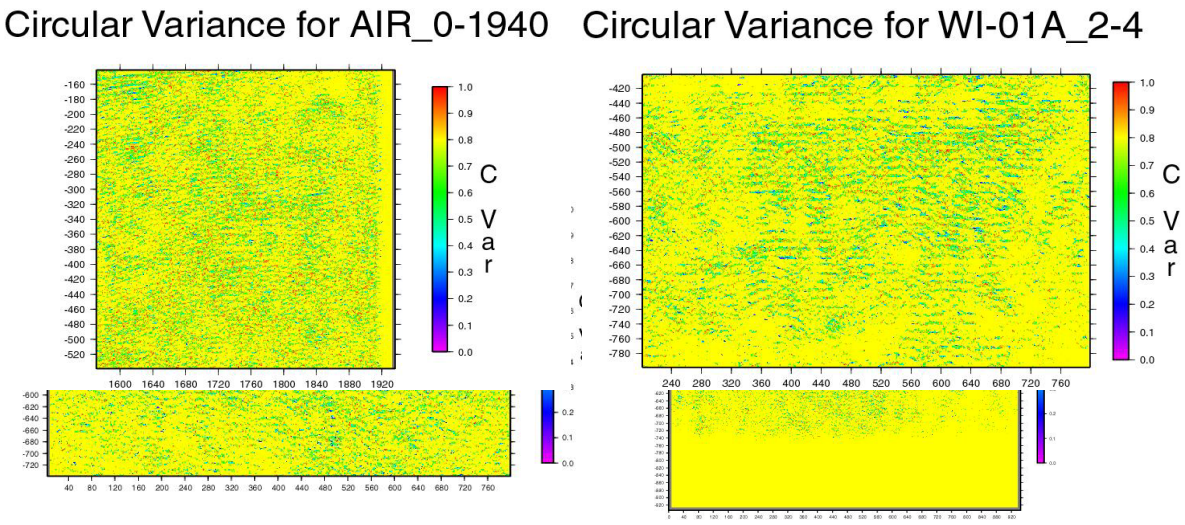

Figure 4.3: *Circular variance plots for sections of AIR-78-88 (top left), WI-01A (top right), WI-01A (bottom left), WI-22 (bottom right) (see text for location), the circular variance have been colour coded to illustrate circular variance per counting circle.*

Circular variance is generally high across the panels as a result of the random scatter of the reflected energy throughout. Localised patches of red (maximum circular variance) are often the result of the counting circle being entirely contained within, or almost full with a particular packer of reflected energy, but the light blue to green colours representing data in the range 0.4-0.7 show a high overall scatter in the data.

4.1.2 Basin Margin

This crustal type is found on both sides of the basin but varies between sides due to the different nature of the structural controls. These areas can be statistically characterised as having dipping vector means which develop moving off the shelf and into the basin. Bands dipping both to the east and west often develop in the upper section of the crust as the analysis picks up uncollapsed fault hyperbolae. Total energy is high and concentrated in bands and circular variance is also high particularly in the upper crust. The two examples shown below are from the eastern margin of the basin where the transition into the basin is relativity sharp. Line 30 shows the transition from the Erris High down into the basin while NWI-21 lies further to the North.

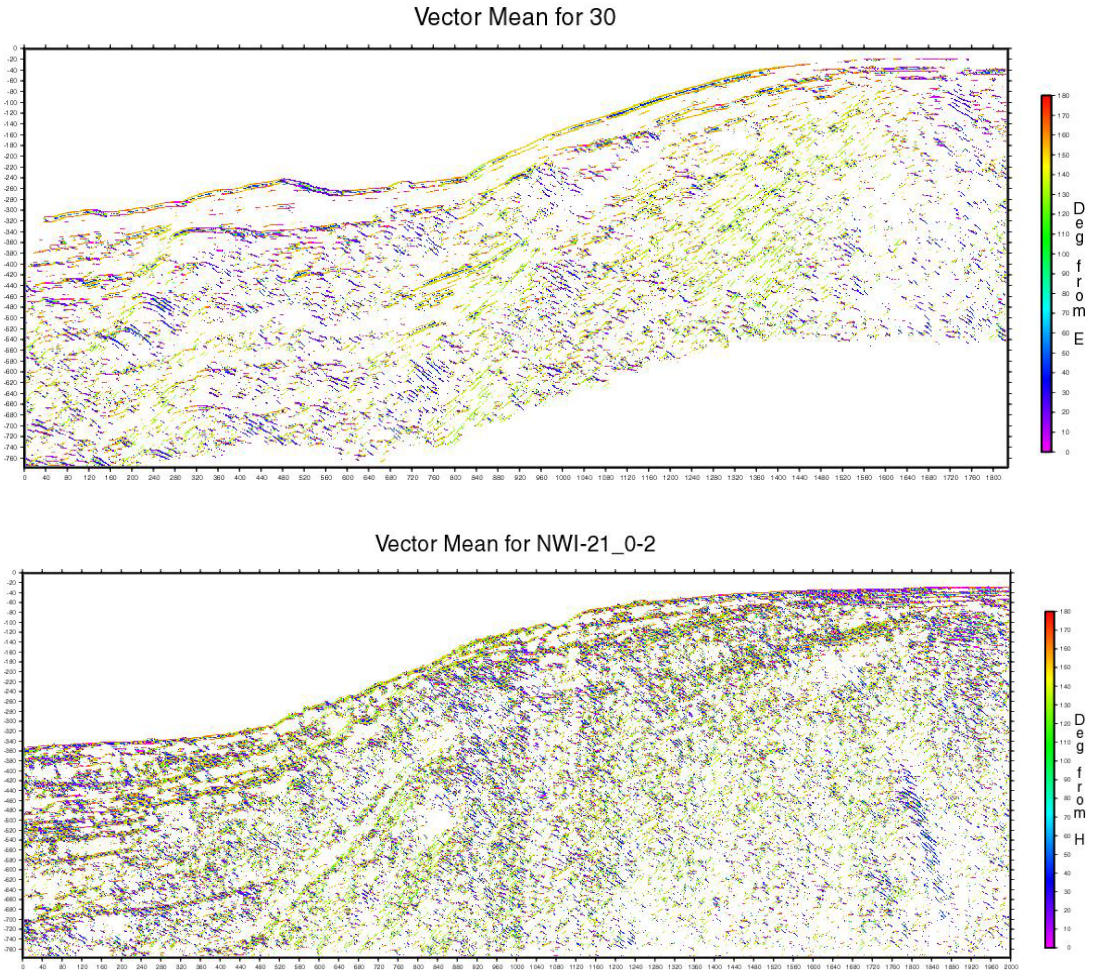

Figure 4.4: *Vector mean plots for sections of Line 30 (top) and the first section of NWI-22 (bottom) (see text for location), the vector means have been colour coded as per the scale bars with orientations increasing clockwise from the horizontal.*

Vector mean for this crustal type shows energy dipping to the east and west as the structure of fault blocks and the internal structure of the blocks themselves is picked out. The area of dominantly green, energy dipping west to the basin is highlighting the common feature of sub horizontal data starting to dip towards the basin as the line draws close to the apex of the margin.

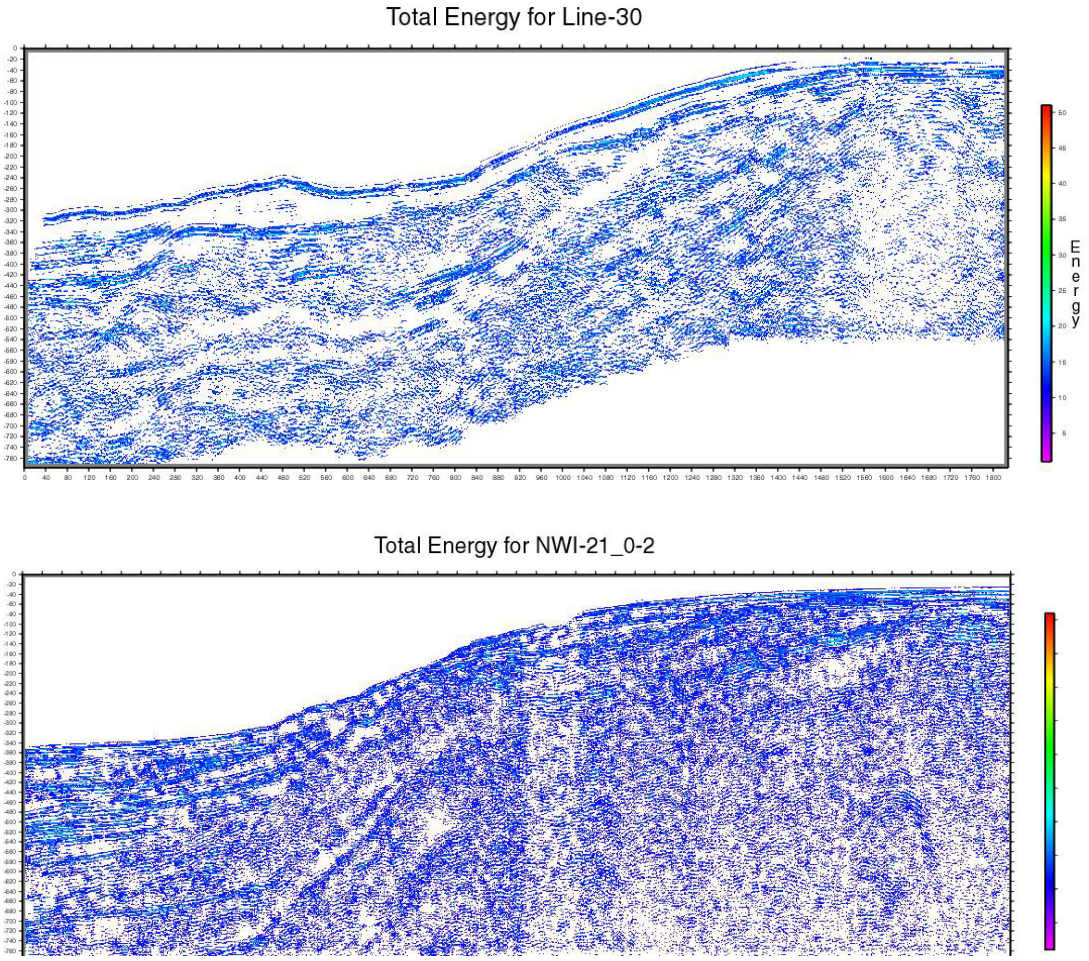

Figure 4.5: *Total energy plots for sections of Line 30 (top) and the first section of NWI-22 (bottom) (see text for location).*

Total energy for this crustal type is medium and becomes concentrated in dipping bands in the margin transition zone, this is best illustrated in Line 30.

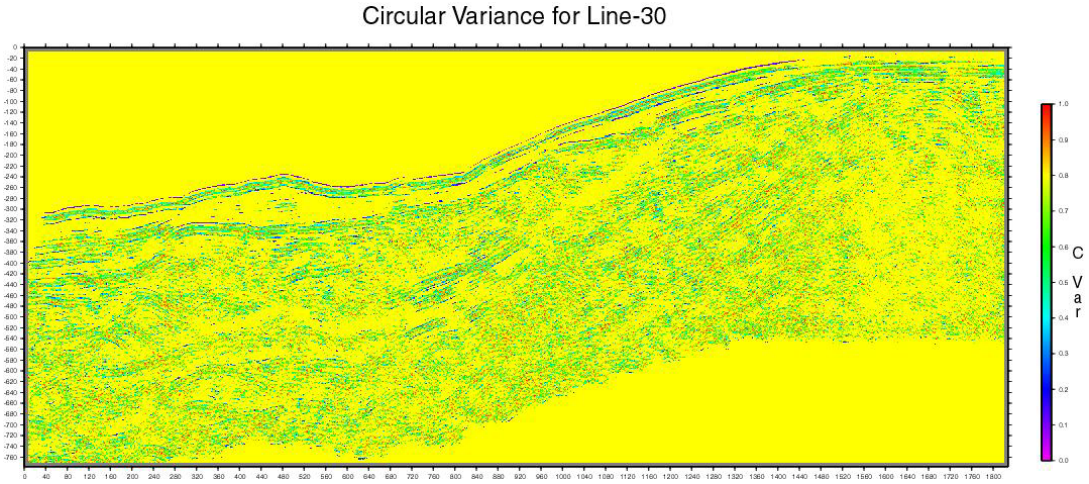

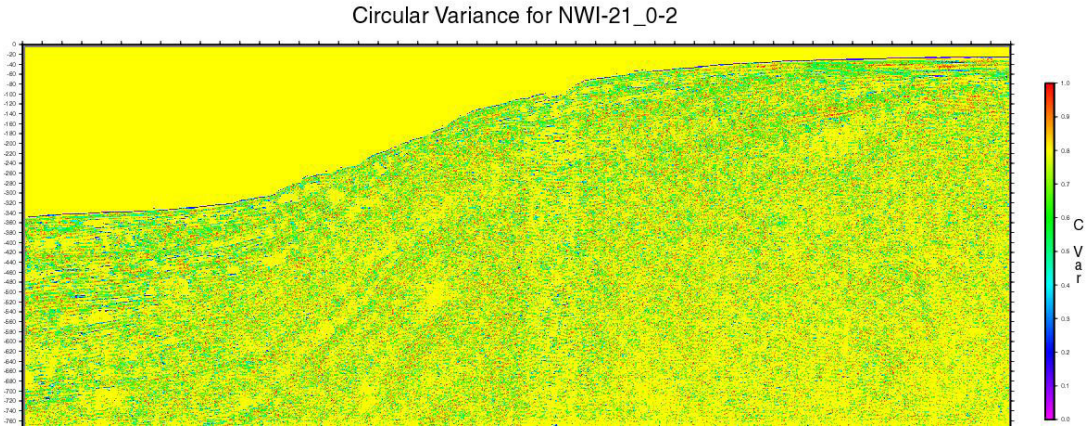

Figure 4.6: *Circular variance plots for sections of Line 30 (top) and the first section of NWI-22 (bottom) (see text for location)*

Circular variance is generally medium to high but can be quite low in dipping bands in the actual margin transition zone.

4.1.3 Thinned Rifted Crust

Thinned rifted crust is seen in the centre of the basin with the upper crust comprising of a thick sequence of sedimentary deposits and the lower crust comprising of the stretched remains of the original crystalline basement. The upper part of this crustal type when analysed shows bands of horizontal vectors representing the flat, acoustically-differentiated sedimentary layers. This banding is picked up again by the energy plots and total energy for this section is generally high. Circular variance is generally low. The lower section again shows bands of predominantly horizontal vectors. These are not as focused as in the upper section but are in strong contrast with the random nature of the vectors in the original crystalline basement. As with the upper crust total energy is high and circular variance low.

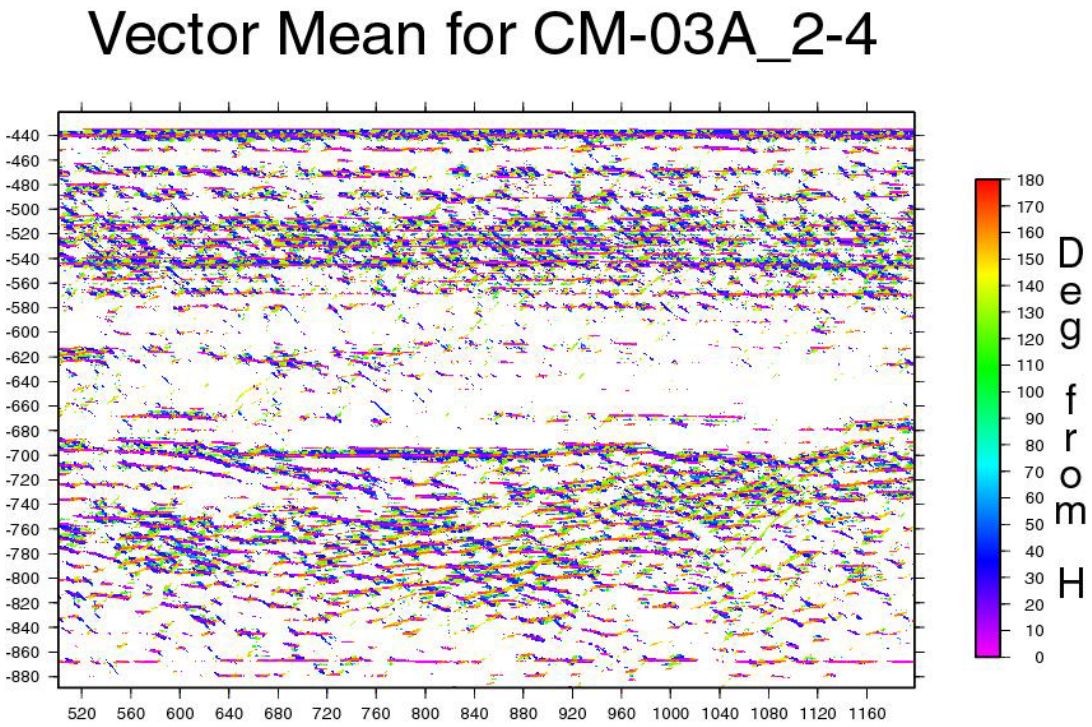

Figure 4.7: *Vector mean plot for sections of CM-03A, see text for location.*

The data here is dominated by sub-horizontal reflections parallel in the upper section and sub-parallel in the lower part. While some of the dipping blue and green energy, particularly in the upper part is due to tying between the parallel reflections (see section 2.1.5), there is also some real westward dipping energy in the bottom right which is due to remnant fault hyberboli.

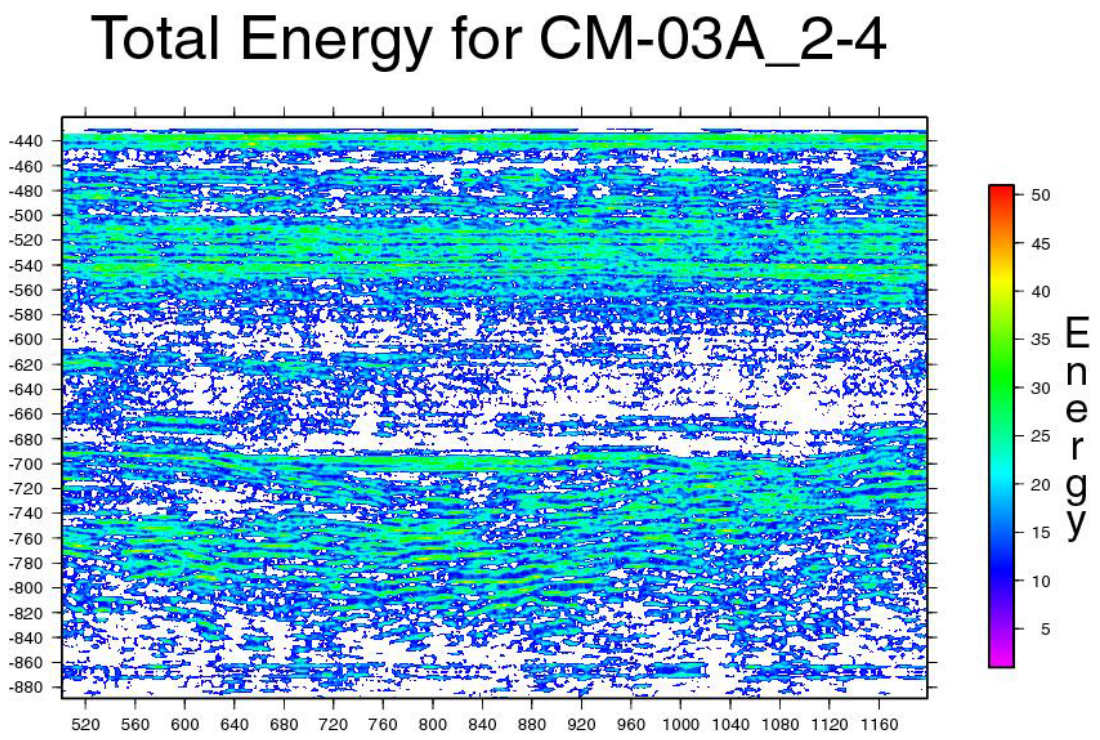

Figure 4.8: *Total energy plot for sections of CM-03A, see text for location.*

Total energy is high and concentrated into distinct horizons.

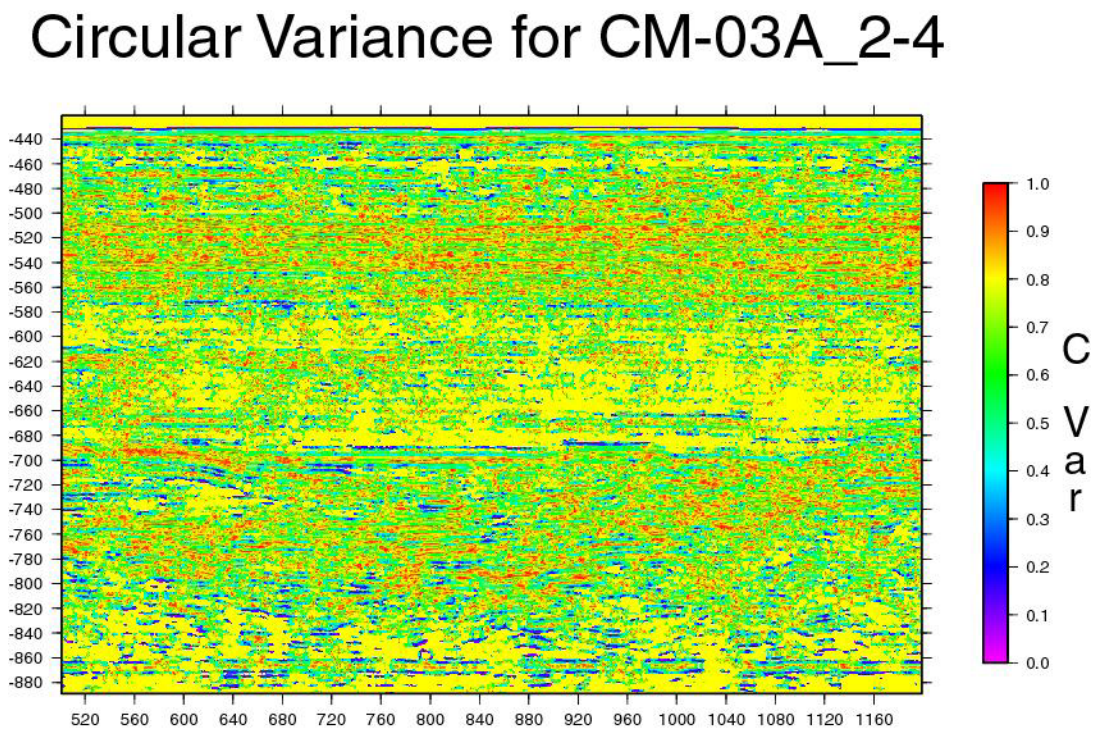

Figure 4.9: *Circular variance plot for sections of CM-03A, see text for location.*

Circular variance is low except in areas where the counting circle has been caught between a glut of data creating an appearance of scatter and giving false high readings, this being a particularly bad section for this problem.

4.2 Strain Ratios

This application builds on work done by Sanderson (1977), on the use of orientation of random lines in two dimensions and the orientations of these lines to quantitatively analyse finite strain. Sanderson essentially took each line as a unit vector and with a given orientation. Each vector was summed. The length of the resultant divided by the size of the data set is a function of the strain the data has undergone assuming a random distribution of the data before strain.

The method works as follows. If you have a data set of originally random lines, the orientation of these lines can be measured, as orientations such as 45^o and 225^o are the same orientations, in the range 0-180 or (0,PI). The angles are then doubled to give a range (0,2PI). Each line is treated as a unit vector. Summing the vectors (already discussed in Section 3.2.2) will give a resultant vector (r) whose direction 0 and magnitude (| r |) give suitable estimates of the mean direction and dispersion of the data. A better description of dispersion is given by | r | / n where n is the sample size, as it is now normalised for the sample size. Since the strain modified uniform distribution, after the doubling of the initial angles, is symmetrical and unimodal the resultant vector is a good estimator of both the mean and mode of such a distribution and independent of the origin of measurements of the angles (Sanderson 1977). Sanderson found | r | / n increased steadily with increasing strain ratios (Rs), and is approximately proportional to ln(Rs) for Rs < 10. Figure 4.11 taken from Sanderson (1977) shows the relationship between ln(Rs) and | r | / n for strain modified uniform distribution.

This method of calculating strain ratio ties in well with VECSTAT as the results of the vector mean analysis give an orientation for each point for which data is present. By taking each one of these data points as a line and therefore as a unit vector, the strain ratio can be calculated as described above.

To check how valid this assumption is, a data set of random orientation was created and strained incrementally. The synthetic data set was then strained incrementally and analysis by VECSTAT at each increment, the vector mean results of this analysis were then used to calculate the strain ratio using the method described above. The initially random data set, required by the assumptions of the method, was created using a series of circles with four internal crosslines dividing the circle into 45^o segments. Each successive circle was then rotated through an angle increasing in one degree increments from $0\text{-}45^o$ to give the full possible range of orientations for the lines (see Figure 4.10).

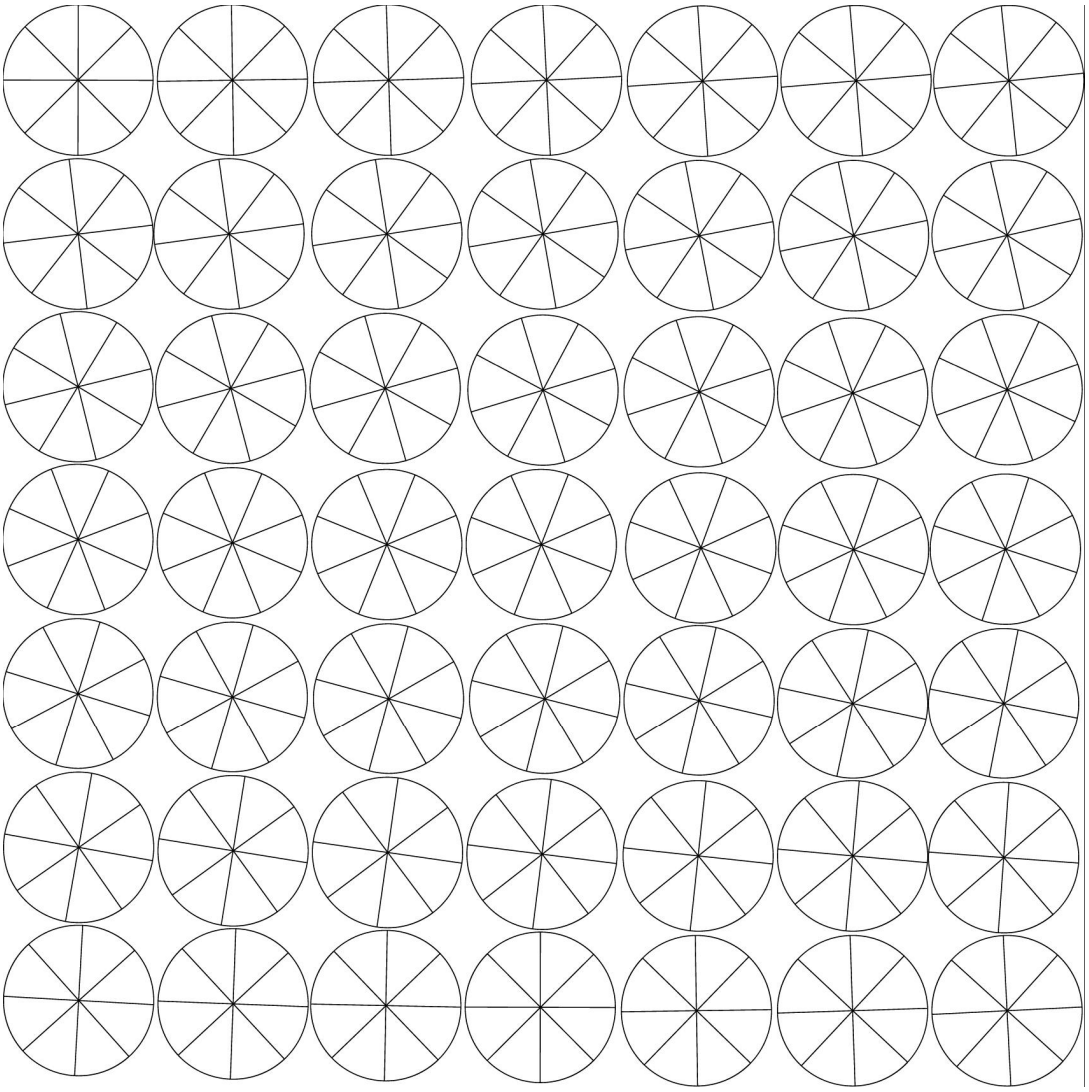

Figure 4.10: *A random data set created using circles divided into 45^o segments, each successive circle is rotated through an incrementally increasing angle in the range 0-45^o, which ensures that there are lines of every orientation present in the data set.*

This data set was then strained in increments, while conserving overall area, the details can be seen in Table 4.1.

X-AXIS	Y-AXIS	RATIO	|R|/N
9	11.11	1.23	0.09
8	12.5	1.56	0.18
7	14.28	2.04	0.28
6	16.66	2.78	0.38
5	20	4	0.49
4	25	6.25	0.69

Table 4.1: *The results of strain analysis using VECSTAT.*

Figure 4.11 shows the comparison between the results from the VECSTAT analysis

and the theoretical results from Sanderson (1977), showing a close match between the two. The lower values found using the VECSTAT method are attributed to confusion in the algorithm in the centre of the circles where the lines intersect introducing random results and thus reducing the value of | r |/ n. The discrepancy increases as the strain increases as the angles between the segments tighten up and a larger area becomes susceptible to interference between the lines. This limit on resolution is common in automatic methods and must be weighed against the fact that the angles need not be calculated by hand. It is hoped that careful application of the circular variance filter will be able to remove this randomness and thus improve the accuracy of the strain measurements.

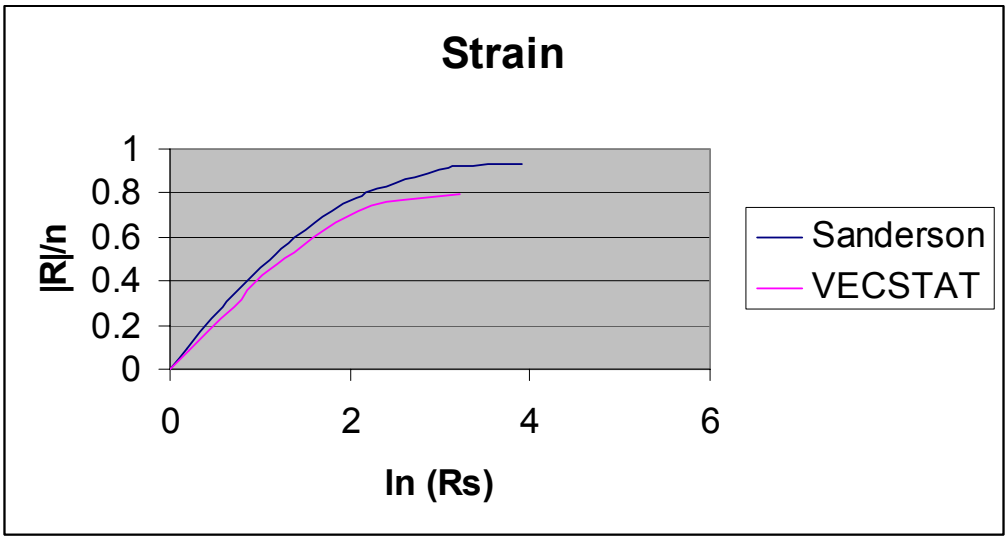

Figure 4.11: *| r | / n Vs ln(Rs) for strain ratios less than ten, results from Sanderson (1977) are replotted in blue while results from VECSTAT are plotted in pink.*

Having seen that VECSTAT's vector mean results can be used to assess strain ratio, is it possible to take this one step further and use this method to assess strain ratio from vector mean analysis of seismic profiles? Several factors have to be considered in undertaking such an analysis

1 *The randomness of the initial data set*: one of the prerequisites for using this method is that the initial data set is random i.e., | *r* | / *n* is zero for an unstrained data set. However as the effect of strain is linear it is possible to compare the degree to which an initially not quite random data set has been stretched by comparing the strain ratio for differently stretched areas of crust. Comparing the strain ratio of the basin margin, therefore, with the strain ration of the basement on the basin floor should reflect the finite strain undergone by that section of the crust.

2 *Homogeneity of the unstretched crust across the area before the basin opened*: If the crust was not the same in the unstretched margin as in basin then it will have a different seismic signature and it is no longer possible to compare them.

3 *Linear increase of the strain ration as seen in the seismic profiles with increased stretching*. This method is not a direct measure of strain but based on seismic profiles. The theory is that as crystalline basement is stretched, there will be a focusing of the random energy found in its profiles as they are strained. In order for this focussing of energy to be correlated with strain ratio it must increase linearly with increasing strain. Clear reflections resulting strong focusing vector means. Therefore the introduction of clear reflections (e.g., igneous bodies), or other factors will cause

incremental increases in the focussing of energy in seismic profiles instead of a linear progression. If this occurs at various stages of the rifting processes it will drastically reduce the accuracy of any strain ratio calculated.

4 *The reflections are real*: a Major assumption is that randomly oriented reflectivity results from simple reflection at linear geological acoustic impedance contrasts and not from wave interference patterns arising from complex heterogeneous geology.

The acquisition of and the processing that is applied to seismic data enhances energy of certain orientations while muting those of other orientations. Stacking gets rid of sub-vertical energy while emphasising sub-horizontal. Migration algorithms applied increase the horizontal continuity of reflections. However, if, as is the case with this application, the two sections being compared are both subject to the same biasing by the processing techniques being applied then the difference between the strain ratio in both can still be compared. To ensure that this is the case, sections from the same line will be used. The sections compared will also be taken from the same depth TWTT as migration techniques applied are usually designed to focus on a particular depth.

Work is continuing on the use of this method to estimate relative strain from seismic sections using data from the Rockall Basin.

4.3 Extracting Orientations

One of the tools available with the suite of programs that perform the analysis of the VECSTAT algorithm is the ability to extract data of a certain orientation. This allows detailed examination of the data present of this orientation. Packages such as the Itogram algorithm (Ryan *et al*., 2000) which calculates the spacing between lineations prefer to work with just one orientation at once. The remaining data can also be examined for patterns and features that have been hidden by the data removed.

Figure 4.12 shows vector mean for test panel comprising of a test panel of fault orientations from a time slice of a 3D seismic data set, and the result of extracting all data oriented 30^{o} ($\pm 7^{o}$) measured clockwise from due east. The extraction of this orientation shows that it is the dominant orientation but that there is also a second smaller population of faults running close to north-south.

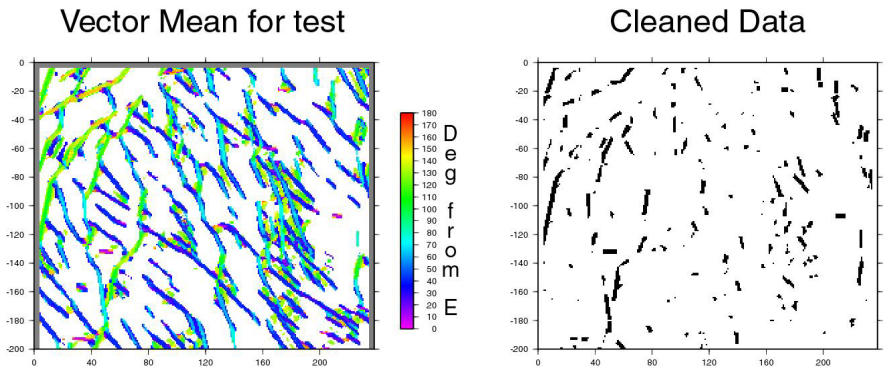

Figure 12: *Left vector mean for a series of faults taken from a 3D time slice, right, data remaining after the removal of the dominant orientation.*

Extractions can also be performed on seismic data, Figure 4.13 shows the effect of extracting data of orientation 120^{o} (Fig. 4.13 bottom left) and 30^{o} (Fig. 4.13 bottom right) from Line 30 (see Fig. 4.4 top). Using this application different reflection packages can be singled out for specific attention.

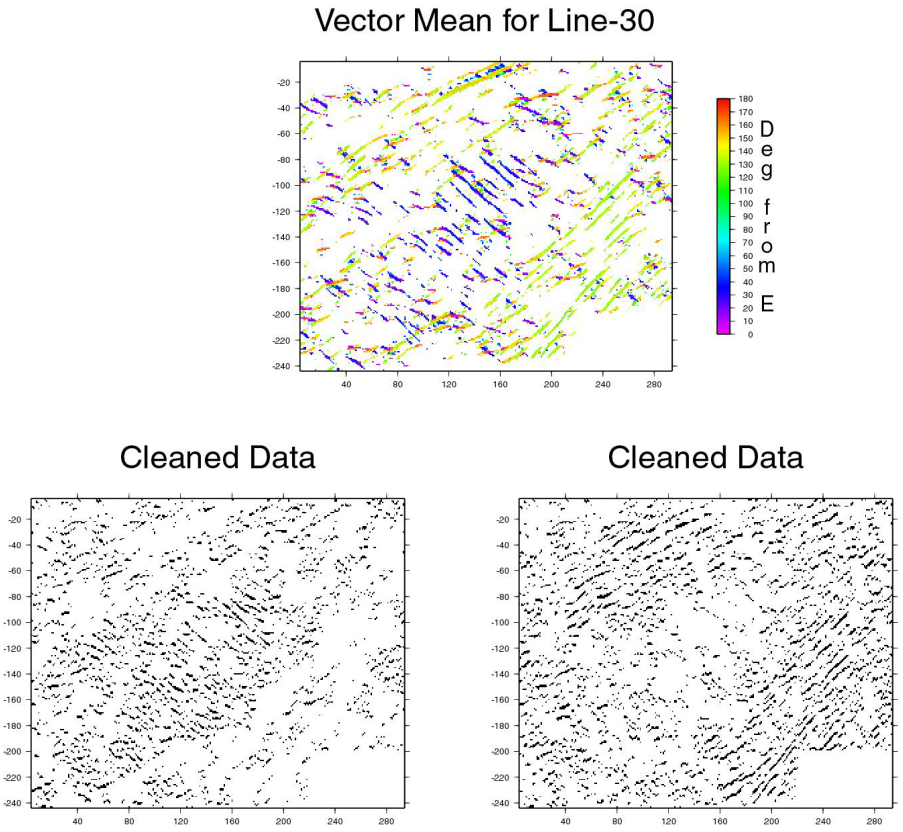

Figure 4.13: *Top, vector mean for a section of Line 30, bottom left data remaining after removal of data of orientation 120^{o} measured clockwise from the horizontal, bottom right data remaining after removal of data of orientation 30^{o}.*

Rockall Data

Some of the seismic profiles used in the study and the results of the statistical analysis by VECSTAT of these lines will now be examined survey by survey. All the profiles were broken into 2000 CMP point segments for analysis

5.1 Survey 70/04

This survey was shot by the GSI in April 1970 as part of an initial investigation of the then Rockall trough, the main acquisition parameters are shown in Table 5.1. The location of the lines used in this study is shown on Figure 5.1. Both lines are perpendicular to the basin margins and transverse the basin with the more southerly Line 1 also imaging part of the Rockall Plateaux.

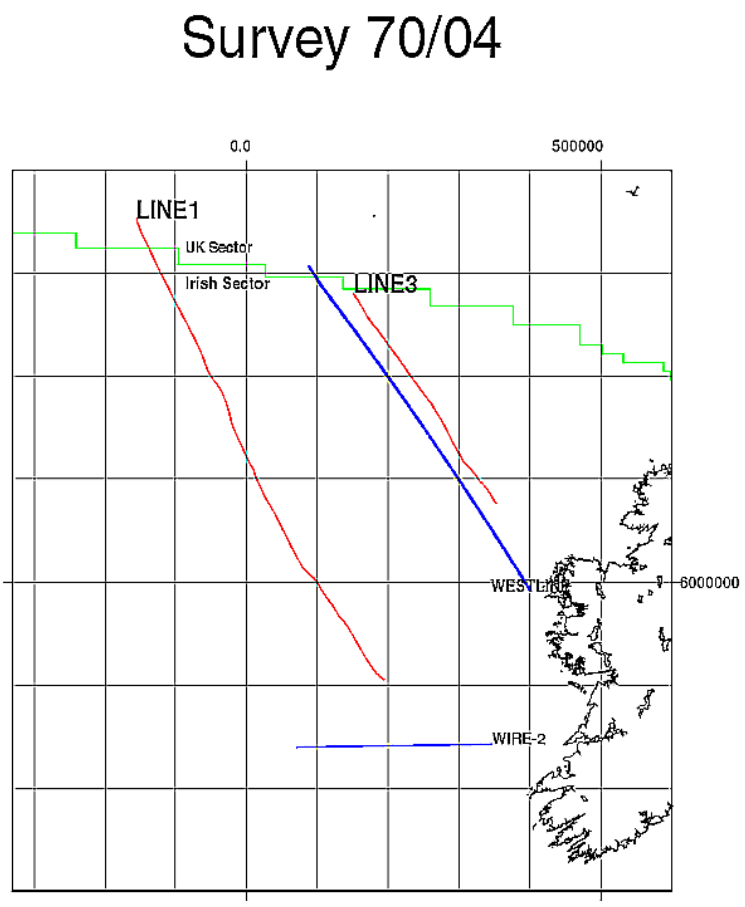

Figure 5.1: *location map showing the lines used in survey 70/04 (red), Westline and Wire-2 have been marked in blue and the boundary between the Irish and UK sectors is delineated in green*

Survey Details	
Survey No.	70/04
Shot by	GSI
Total Survey length	1145 km
Source	Airguns (900 cu. in.)
Source Depth	30'
SP interval	50 m

Survey Details	
Streamer length	2400 m
No of Group	24
Group interval	100 m
Processing	TV, DBS, 2400% stack, TVDAS,TVF
Vertical scale	5 cm/sec
Horizontal scale	1:47,520
Line number and SP range	LINE 1 SP 3120-5820
Line number and SP range	LINE 3 SP 5821-7250

Table 5.1: *Selected acquisition parameters from Survey 70/04.*

5.1.1 LINE 1

This 566.35 km line starts on the south eastern part of the Hatton High before dipping into the Hatton Basin and across the Rockall Bank. Once in the Rockall Basin itself it crosses two northerly expressions of the Barra Volcanic Ridge system. It leaves the basin in the east via the marginal Macdara Basin and Stifin High (Naylor *et al.* 1999). The line ends on the Porcupine High. The line starts with poor penetration and quality of data with strong multiples obscuring any information present in the basement. Data quality and penetration increase as the line crosses the Rockall Basin and improves again as on the Porcupine high where 5 sec of basement is imaged. The key parameters used by VECSTAT are Detailed in Table 5.2.

VECSTAT Parameters	
Long axis / counting circle radius	10
Short axis	2
Total filled pixels	12

Table 5.2: *Key parameters used by VECSTAT in analysing LINE 1.*

The results of VECSTAT's analysis of the line are presented in Table 5.3. GMT plots of the results are on CD-ROM 1:/survey70-04/line1/line1vec.pdf, line1eng.pdf, line1var.pdf.

CMP Range	Vector Mean	Circular Variance	Total Energy	Crustal Type	|r|/n	Comments
0-560	Random	V. high	High/ diffuse	Unst.	0.38[a]	
560-3320	Random	V. high	Medium/ diffuse	Unst.	0.29[b]	Overlain by sedimentary sequence
3320-5400	Random	V. high	Medium/ diffuse	Unst.		Strong Multiples
5400-5800	Dipping	Medium	High/ Focused	Margin	0.184[c]	
5800-8860	Parallel sub-horizontal closely spaced	Low	medium	Inferred as stretched continental		No basement
8860-9400	Dipping	Medium	High/	Margin		

CMP Range	Vector Mean	Circular Variance	Total Energy Focused	Crustal Type	|r|/n	Comments

Table 5.3: *The results of VECSTAT's statistical analysis of LINE1 divided into sections on the basis of crustal types. The sections used for |r|/n analysis are outlined on CD-ROM 1:/survey70-04/line1/line1vec.pdf and labelled a,b,c as the results. Unst. = unstretched basement.*

A shallow sedimentary basin begins at CMP 560 with sub-horizontal reflections termination in a random noisy section illustration an unlapping sequence. The basin thickens 1 sec TWTT with the sedimentary sequence resting unconformably on an undulating subsurface. The absence of transition zones showing statistical characteristics typical of a basin margin on either side of this basin gradual nature of the margins of the basin.
Evaluation of |r|/n on the Rockall Bank (CMP 3320-5400) was not possible due to the presence of many strong multiples which left bands of true data that were to narrow to analyse properly.
CMP 5400 sees a change to margin characteristics with sedimentary layers present by CMP 5840. The parallel horizontal vector means thicken quickly to 3-3.5 sec TWTT which comprises almost all that is imaged beneath the deep water column in the part of the line within the Rockall Basin itself. Two steep domes clouded in dipping defracted energy, interpreted as northerly extensions of the Barra volcanic ridges (Naylor *et al.* 1999) are present at CMPs 7320 and 7990. At CMP 8860 a lower layer of week and uncontinuos sub-horizontal vector means quickly passes to random unstretched crust vector means marking the end of the basin.
On the Porcupine High (approx. CMP 10340) the vector mean analysis images a considerable amount of sub horizontal energy in the upper 2 sec TWTT of the section. This is unusual for basement highs which usually have a characteristic random vector mean pattern.

5.1.2 LINE 3

This 286.99 km line starts on the Rockall Bank and enters the Rockall basin via the Ronan Basin and the Ladra High (Naylor *et al*. 1999) It then crosses an area of thick sills and continues to the eastern side of the basin. Data quality and penetration is reasonably good on the Rockall Bank and the western margin. Penetration is however hampered by the presence of thick sills on the western side of the basin.

Processing Parameters	
Long axis / counting circle radius	10
Short axis	2
Total filled pixels	15

Table 5.4: *Key parameters used by VECSTAT in analysing LINE3.*

The results of VECSTAT's analysis of the line are presented in Table 5.5. GMT plots of the results are on CD-ROM 1:/survey70-04/line3/line3vec.pdf, line3eng.pdf, line3var.pdf.

CMP Range	Vector Mean	Circular Variance	Total Energy	Crustal Type	|r|/n	Comments
0-300	Random	V. high	High/ diffuse	Unst.	0.12[a]	
300-1780	Dipping	Medium	High Focused	Margin	0.21[b]	
1780-1980	Parallel sub-horizontal closely spaced	Medium	Medium /focused	Margin		Perched basin
1980-5720	Parallel sub-horizontal closely spaced	Medium	High/ focused	Basin with igneous intrusion		

Table 5.5: *The results of VECSTAT's statistical analysis of LINE3 divided into sections on the basis of crustal types. The sections used for |r|/n analysis are outlined on CD-ROM 1:/survey70-04/line3/line3vec.pdf and labelled a,b as in the table.*

The line quickly moves from the unstretched basement of the Rockall Bank to the basin margin. The margin zone the dipping nature of the vector means is somewhat amplified by the effect of multiples of the sediment water interface.
CMP 1880 marks the centre point of a small perched basin with sub-horizontal parallel vector means down to 6.4 sec TWTT. Once in the Rockall Basin itself very little basement is imaged and penetration is hampered by igneous sills.

5.2 Survey 72/07

This survey was shot by Western Geophysical in August 1972, the main acquisition parameters are shown in Table 5.6. The location of the one line used in this study is shown on Figure 5.2.

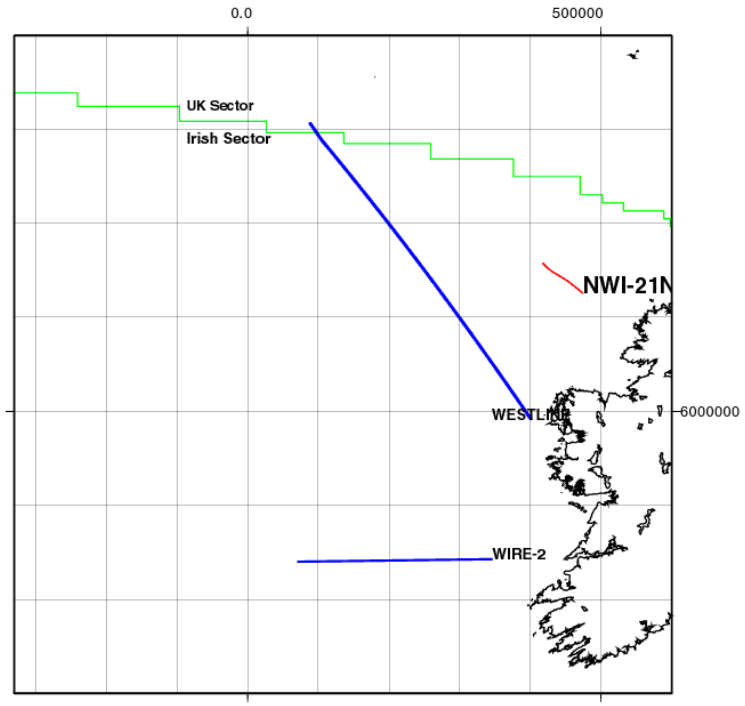

Figure 5.2: *location map showing the lines used in survey 71/07 (red), Westline and Wire-2 have been marked in blue and the boundary between the Irish and UK sectors is delineated in green.*

Survey Details	
Survey no.	72/07
Shot by	Western Geophysical
Total Survey length	1568 km
Source	Maxipulse (0.5 lb)
Source Depth	40-50'
SP interval	-
Streamer length	2400 m
No of Groups	48
Group interval	50 m
Processing	DBS, 2400% stack, DAS, TVF
Vertical scale	5 cm/sec
Horizontal scale	1:30,000
Line number and SP range	NWI-21NW SP 300-618

Table 5.6: *Selected acquisition parameters from Survey 72/07.*

5.2.1 NWI-21NW

This 65.54 km line runs from west to east, across the eastern margin of the Rockall Basin, across the Erris High into the Erris Basin. The line shows fair to good quality data with penetration increasing a it moves out of the basin.

Processing Parameters	
Long axis / counting circle radius	10
Short axis	2
Total filled pixels	10

Table 5.7: *Key parameters used by VECSTAT in analysing NWI-21NW.*

The results of VECSTAT's analysis of the line are presented in Table 5.8. GMT plots of the results are on CD-ROM 1:/survey72-07/NWI-21NW/NWI-21vec.pdf, NWI-21eng.pdf, NWI-21var.pdf.

CMP Range	Vector Mean	Circular Variance	Total Energy	Crustal Type	|r|/n	Comments
0-480	Sub-horizontal	Medium	High/ focused	Basin		Inferred
480-1200	Dipping	Medium	Medium/ focused	Margin	0.31[a]	Unmigrated energy
Upper 1200-1600	Dipping	low	Medium/ Focused	Margin	0.35[b]	
lower	Random	Medium	low/ diffuse	Unst.	0.33[c]	
1600-2590	Random	Medium	low/ diffuse	Unst.		

Table 5.8: *The results of VECSTAT's statistical analysis of NWI-21NW divided into sections on the basis of crustal types. The sections used for \|r\|/n analysis are outlined on CD-ROM 1:/survey72-07/NWI-21NW/NWI-21vec.pdf and labelled a,b,c as in the table.*

From the start of the line to CMP 480 very little basement is imaged beneath a sedimentary section which increases in thickness westwards to 2.5 sec TWTT and has closely spaced vector means. From this small section it was not possible to identify this section as belonging to any particular crustal group but from its location w.r.t following sections of the line and its deep bathymetric expression it was inferred as thinned stretched crust.
The next part of the line, CMP 480-1200 has a clearly marginal crustal characteristics for unmigrated or poorly migrated data. Vector means are in general dipping to the east or west with orientations predominantly in the 20-40^{o} and 100-130^{o} ranges (orientations measured clockwise from the horizontal). Total energy is medium and concentrated in dipping bands. From CMP 1200 the lower part of the line shows random vector means and typical characteristics of unstretched crystalline basement however bands of dipping vector mean continue in the upper 2 sec TWTT until CMP 1600.

5.3 Survey 75/03

This survey was shot by CGG in March 1975, the main acquisition parameters are shown in Table 5.9. The locations of the lines from this survey used in this study are shown on Figure 5.3. Both lines run from the Erris Basin across the Erris high into the Rockall Basin.

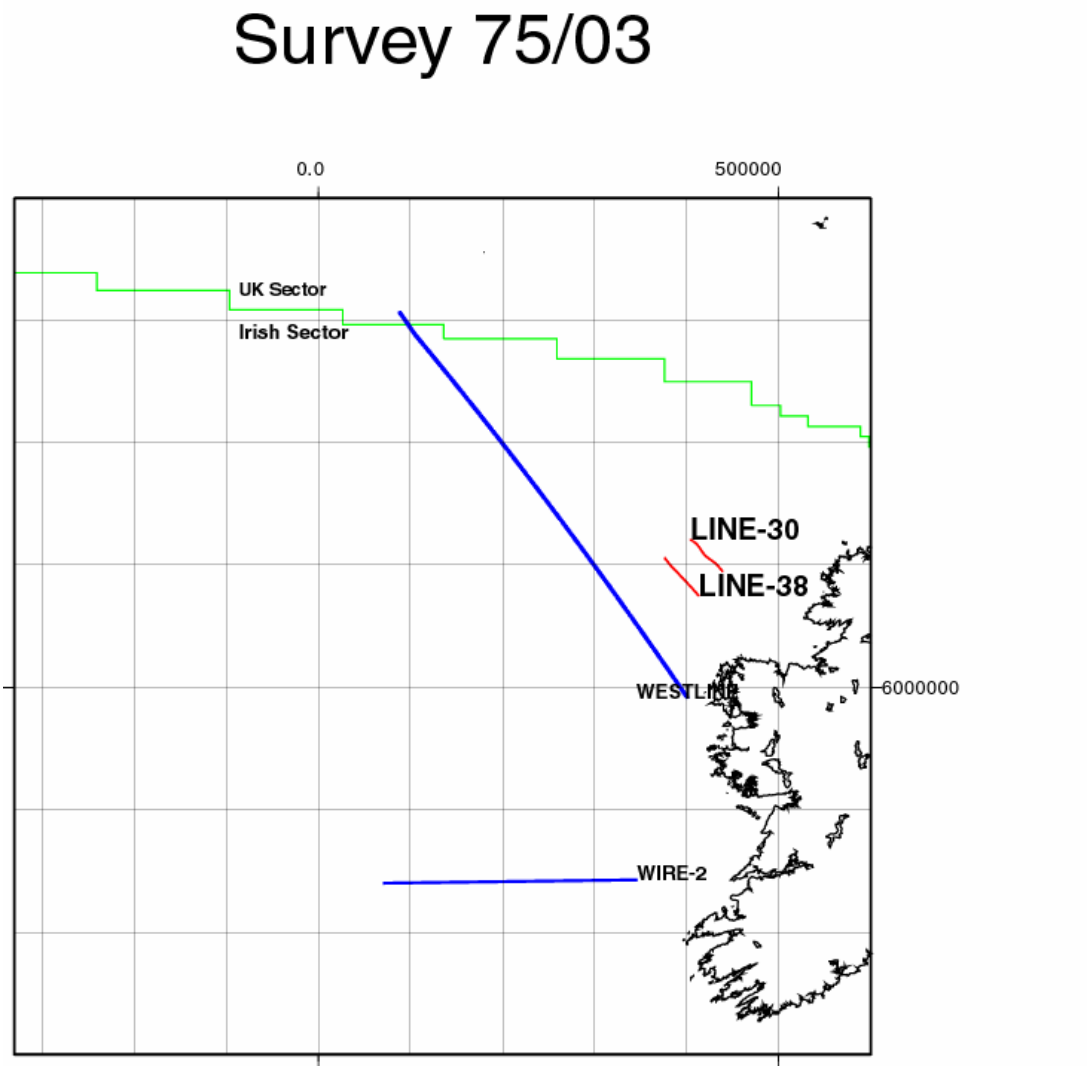

Figure 5.3: *location map showing the lines used in survey 75/03 (red), Westline and Wire-2 have been marked in blue and the boundary between the Irish and UK sectors is delineated in green.*

Survey Details	
Survey No.	75/03
Shot by	CGG
Total Survey length	1561 km
Source	Vaporchoc
Source Depth	
SP interval	-
Streamer length	2400 m
No of Groups	48
Group interval	50 m
Processing	DBS, 4800% stack, DAS, TVF
Vertical scale	3.75 "/sec

Survey Details	
Horizontal scale	N/A
Line number and SP range	LINE 30 SP 1-1608
Line number and SP range	LINE 38 SP 1-1760

Table 5.9 *Selected acquisition parameters from Survey 75/03.*

5.3.1 LINE-30

This 44.04 km line starts in the Rockall Basin moving up onto the Irish shelf. The data is of good quality with penetration increasing as the line climbs onto the shelf

Processing Parameters	
Long axis / counting circle radius	10
Short axis	2
Total filled pixels	10

Table 5.10: *Key parameters used by VECSTAT in analysing LINE-30*

The results of VECSTAT's analysis of the line are presented in Table 5.11. GMT plots of the results are on CD-ROM 2:/survey75-03/line30/line30vec.pdf, line30eng.pdf, line30var.pdf.

CMP Range	Vector Mean	Circular Variance	Total Energy	Crustal Type	|r|/n	Comments
0-1600	dipping	Medium-low	Medium-low/ focused	Margin	0.43	Very clear dipping vector means

Table 5.11: *The results of VECSTAT's statistical analysis of LINE-30 divided into sections on the basis of crustal types. The entire section was used for |r|/n analysis.*

Line 30 provides a very nice example of the Margin crustal type thanks to the good quality of the seismic data. Despite some confusion occurring between closely space parallel reflections the vector means of the individual reflections a clearly picked out. The |r|/n assessment was done using the whole line.

5.3.2 LINE-38

This 48.7 km line to the south west of LINE-30 again images the transition from the basin to the trough. The profile shows good penetration with increasing basement content as the line moves onto the shelf.

Processing Parameters	
Long axis / counting circle radius	10
Short axis	2
Total filled pixels	10

Table 5.12: *Key parameters used by VECSTAT in analysing LINE-38.*

The results of VECSTAT's analysis of the line are presented in Table 5.13. GMT plots of the results are on CD-ROM 2:/survey75-03/line38/line38vec.pdf, line38eng.pdf, line38var.pdf.

CMP Range	Vector Mean	Circular Variance	Total Energy	Crustal Type	|r|/n	Comments
0-320	Sub-horizontal	Low	Medium/ focused	Basin		Clean data
320-1965	dipping	Low	Medium Focused	Margin		Unmigrated energy

Table 5.13: *The results of VECSTAT's statistical analysis of LINE-38 divided into sections on the basis of crustal types.*

The line starts with basin type characteristics but these halt abruptly at CMP 320 with some of the upper sedimentary layers clearly offset. This is followed by dipping vector means characteristic of basin margins. There is some unmigrated energy present but the data is generally clean.

5.4 Survey 75/07

This survey was shot by Western Geophysical in May 1975, the main acquisition parameters are shown in Table 5.14. The locations of the lines from this survey, used in this study are shown on Figure 5.4.

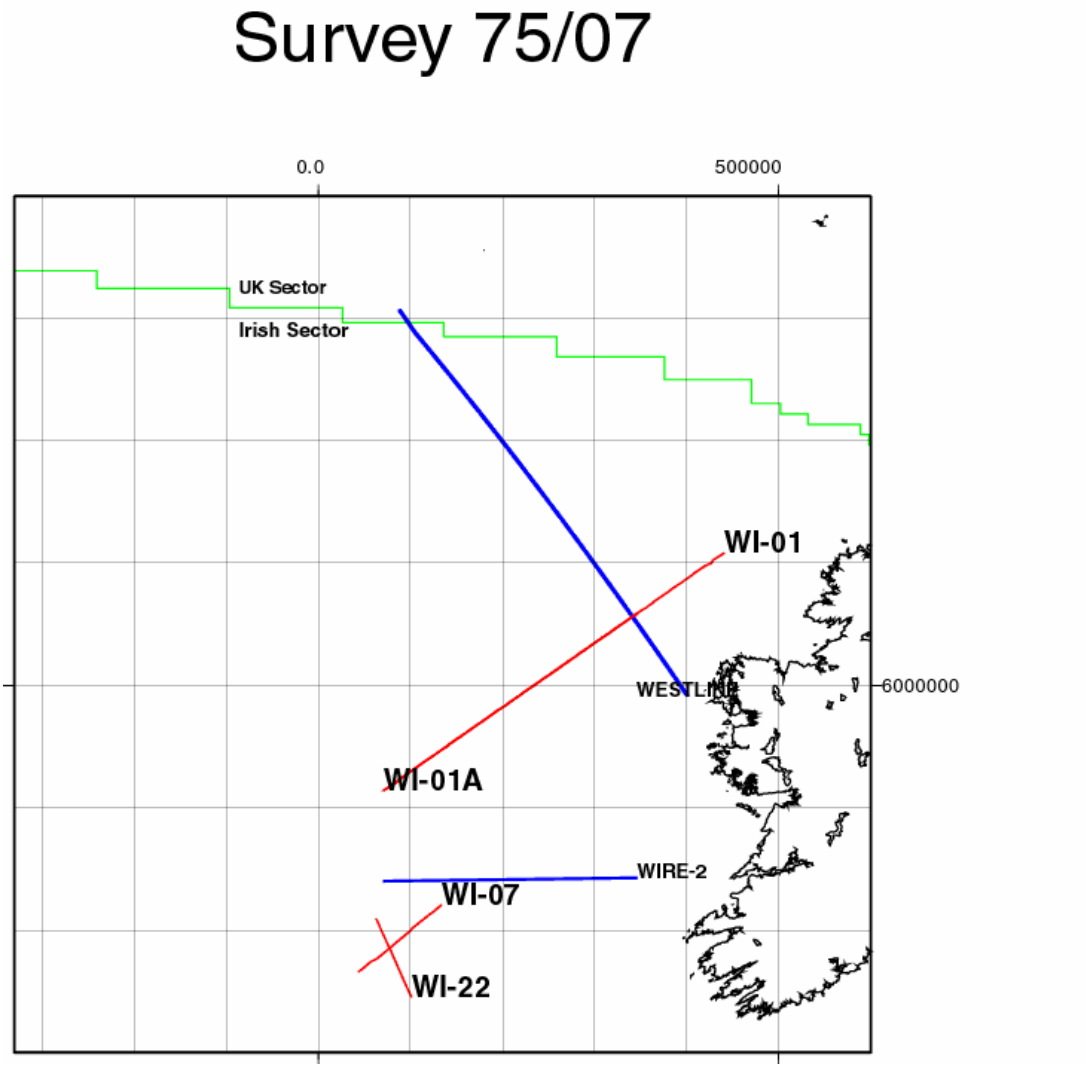

Figure 5.4: *location map showing the lines used in survey 75/07 (red), Westline and Wire-2 have been marked in blue and the boundary between the Irish and UK sectors is delineated in green.*

Survey Details	
Survey No.	75/07
Shot by	Western Geophysical
Total Survey length	5854 km
Source	Maxipulse (8 oz ncn)
Source Depth	40 '
SP interval	200 m
Streamer length	2400 m
No of Groups	48
Group interval	50 m
Processing	DBS, 2400% stack, DAS, TVF
Vertical scale	5 cm/sec
Horizontal scale	1:80,200
Line number and SP range	WI-01 SP 1-559
Line number and SP range	WI-01A SP 1-1558
Line number and SP range	WI-07 SP 370-890

Survey Details	
Line number and SP range	WI-22 SP 600-968

Table 5.14: *Selected acquisition parameters from Survey 75/07.*

5.4.1 WI-01

This 105.38 km line runs north east from the Rockall Basin passing south of the Erris High into the Erris Basin. Good penetration and data quality throughout with up to 6 sec of basement imaged.

Processing Parameters	
Long axis / counting circle radius	10
Short axis	2
Total filled pixels	10

Table 5.15: *Key parameters used by VECSTAT in analysing WI-01.*

The results of VECSTAT's analysis of the line are presented in Table 5.16. GMT plots of the results are on CD-ROM 2:/survey75-07/WI-01/WI-01vec.pdf, WI-01eng.pdf, WI-01var.pdf.

CMP Range	Vector Mean	Circular Variance	Total Energy	Crustal Type	|r|/n	Comments
0-1200	Dipping	Low-medium	Low/ focused	Margin		Undulating surface to sediment/water interface
1200-2180	Dipping	Low-medium	Low/ Focused	Margin		Cuts margin at an oblique angle
2180-3000	Sub-horizontal closely spaced	low	Medium/ Focused	Basin		
3800-4558	Random	Medium-high	Low/ diffuse	Unst.		Very little energy

Table 5.16: *The results of VECSTAT's statistical analysis of WI-01 divided into sections on the basis of crustal types.*

There are two important points to consider when examining this line. The line cuts the margin at a very low angle and there is very little noise in the analysed section. There is some doubt as to the nature of the first section up to CMP 1200 but it has been attributed as marginal due to its dipping vector means. From 1200-2180 is typical of marginal types but with shallower dips due to the oblique angle the line makes with the orientation of the margin. Circular variance is low due to the concentration of the energy into dipping bands. |r|/n was not analysed as when dealing with margins it is only valid perpendicular to the sides of the basin (see section 4.2).

The upper section of CMP 2180 to 3000 has all the characteristics of sedimentary fill with closely spaced parallel sub-horizontal vector means representing the southern part of the Erris Basin.
From CMP 3000 we see a return to marginal characteristics as the line climbs out of the Erris Basin and onto the Irish shelf, at about CMP 3800. On the shelf Total energy is low due to the quiet nature of the data but the distribution is still very diffuse as expected when analysing random energy.

5.4.2 WI-01A

This 311.03 km extension of WI-01 continues where the it left off in the Rockall Basin intersecting obliquely with the north west conner of the Porcupine High before moving rapidity into the Macdara basin and back down into the Rockall Basin. The quality of the data while poor initially improves as water dept decreases.

Processing Parameters	
Long axis / counting circle radius	10
Short axis	2
Total filled pixels	10

Table 5.17: *Key parameters used by VECSTAT in analysing WI-01A.*

The results of VECSTAT's analysis of the line are presented in Table 5.18. GMT plots of the results are on CD-ROM 2:/survey75-07/WI-01A/WI-01Avec.pdf, WI-01Aeng.pdf, WI-01Avar.pdf.

CMP Range	Vector Mean	Circular Variance	Total Energy	Crustal Type	|r|/n	Comments
Upper 0-1320	Parallel sub-horizontal	Medium-low	High /V. focused	Basin		
lower	Scattered	Medium-low	Medium focused			
1320-2080	Dipping	Low-medium	Low/ focused	Margin		
2080-7900	Random	High	Medium/ diffuse	Unst.	0.38[a] 0.431[b] 0.39[c]	
7900-9240	Dipping	Low-medium	Low Focused	Margin		
Upper 9240-12560	Parallel sub-horizontal	Medium-low	High /V. focused	Basin		Lots of faulting
Lower	Scattered	Medium-low	Low focused			

Table 5.18: *The results of VECSTAT's statistical analysis of WI-01A divided into sections on the basis of crustal types. The sections used for \|r\|/n analysis are outlined on CD-ROM 2:/survey75-07/WI-01A/WI-01Avec.pdf and labelled a,b,c as in the Table.*

The line starts at the same point as WI-01 in the Rockall basin but heads south to the Porcupine High. It shows basin characteristics until CMP 1320 with sedimentary

layers and poor penetration of the basin. A short margin sequence then follows to CMP 2080.
The Porcupine High where crossed by this line is divided into two blocks of unstretched basement separated a deep (1 sec TWTT) surface depression centred on CMP 2880. While both sides of the depression show random vector means total energy is much higher on the northern side (CMP range 2080-2880). CMP 7000 sees the introduction of strong multiples. From CMP 7900 the line begins an oblique descent back into the Rockall basin.

5.4.3 WI-07

This 105.38 km line runs from the Rockall Basin north east across the Cliona High into the South Brona Basin. From there it crosses onto the Porcupine High. The quality of the data is good throughout with good basement penetration.

Processing Parameters	
Long axis / counting circle radius	10
Short axis	2
Total filled pixels	10

Table 5.19: *Key parameters used by VECSTAT in analysing WI-07.*

The results of VECSTAT's analysis of the line are presented in Table 5.20. GMT plots of the results are on CD-ROM 2:/survey75-07/WI-07/WI-07vec.pdf, WI-07eng.pdf, WI-07var.pdf.

CMP Range	Vector Mean	Circular Variance	Total Energy	Crustal Type	|r|/n	Comments
0-440	Closely spaced sub-horizontal	Medium	High/ focused	Basin		No data below sediments.
440-920	No Data	No Data	No data	Inferred margin onto Cliona High		
Upper 920-1400	Closely spaced sub-horizontal sub-random	Low-medium	High/ focused	Basin	0.43[a]	
Lower 1400-2720	Dipping	Medium	High/ diffuse Medium/ focused	Margin		Cuts obliquely
2720-4161	Random	High	Medium/ diffuse	Unst.	0.26[b]	

Table 5.20: *The results of VECSTAT's statistical analysis of WI-07 divided into sections on the basis of crustal types. The sections used for \|r\|/n analysis are outlined on CD-ROM 2:/survey75-07/WI-07/WI-07vec.pdf and labelled a,b as in the Table.*

The line starts just inside the basin with characteristic sedimentary vector means abutting against what is inferred to be the marginal step up to the Cliona High and the

high itself, there is no useful data below the sedimentary cover in this section (CMP 440-920).
The line then crosses a small sedimentary basin (South Brona). Vector means below the basin are fairly random but some lineations are present. Total energy is diffuse characteristic of crystalline basement.
CMP 1400-2720 is taken as an oblique cut of a margin sequence but data is scarce and there is some inference here. CMP 2720 marks the start of definite unstretched basement.

5.4.4 WI-22

This 75.21 km line runs southeast from the edge of the Cliona High through the South Brona and Cillian Basins. Then it traverses the Porcupine High. The data is poor in quality at first with multiples affecting deeper parts. It does improve in the shallower waters of the Porcupine High however.

Processing Parameters	
Long axis / counting circle radius	10
Short axis	2
Total filled pixels	10

Table 5.21: *Key parameters used by VECSTAT in analysing WI-22.*

The results of VECSTAT's analysis of the line are presented in Table 5.22. GMT plots of the results are on CD-ROM 2:/survey75-07/WI-22/WI-22vec.pdf, WI-22eng.pdf, WI-22var.pdf.

CMP Range	Vector Mean	Circular Variance	Total Energy	Crustal Type	|r|/n	Comments
0-1320	Dipping Bands	Low	High/ focused	Margin		Strong multiples
1320-1800	Dipping	Low	Low/ focused	Margin		Large controlling Fault
1800-2900	Random	High	Low/ diffuse	Unst.	0.11	

Table 5.22: *The results of VECSTAT's statistical analysis of WI-22 divided into sections on the basis of crustal types. The sections used for \|r\|/n analysis are outlined on CD-ROM 2:/survey75-07/WI-22/WI-22vec.pdf and labelled a.*

Up to CMP 1320 is considered to be a block of unstretched basement (Cliona High) but the statistical characteristics have been obliterated by strong dipping multiples. This is followed by the South Brona Basin bounded by what must be a major controlling fault on its Eastern margin. To the east again lies unstretched basement with a blanket of sedimentation on top.

5.5 Survey 77/09

This survey was shot by S & A Geophysical in August 1977 , the main acquisition parameters are shown in Table 5.23. The locations of the lines used in this study is shown on Figure 5.5. The survey consists of a series of axial profiles contained entirely within the Rockall Basin.

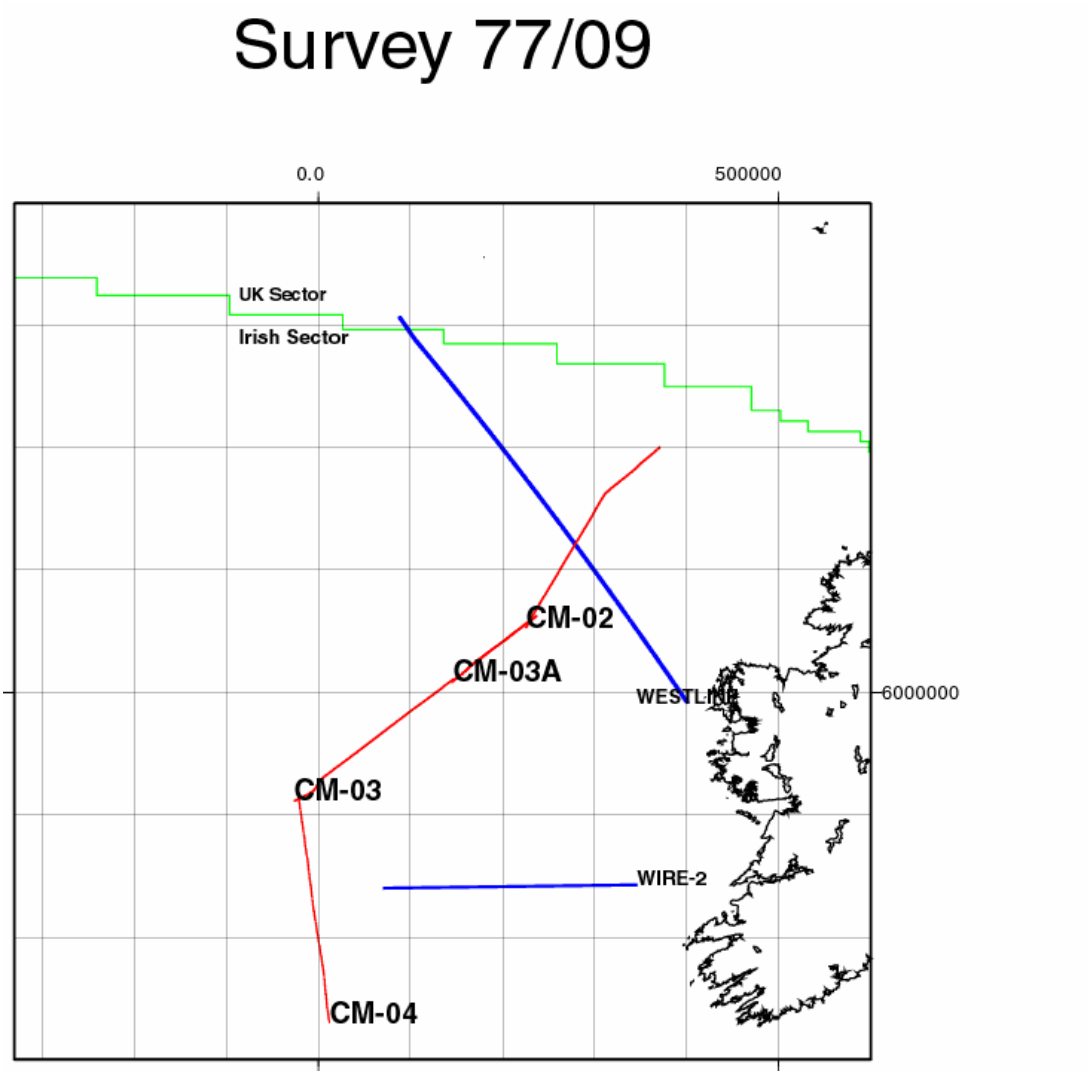

Figure 5.5: *location map showing the lines used in survey 77/09 (red), Westline and Wire-2 have been marked in blue and the boundary between the Irish and UK sectors is delineated in green.*

Survey Details	
Survey no.	77/09
Shot by	S & A Geophysical
Total Survey length	4345 km
Source	7 Airguns (1511 cu. in. 1800 psi)
Source Depth	8 +/- 1 m
SP interval	50 m
Streamer length	2400 m

Survey Details	
No of Groups	48
Group interval	50 m
Processing	DBS, 2400% stack, DAS, TVF
Vertical scale	5 cm/sec
Horizontal scale	1:50,000
Line number and SP range	CM-02 SP 10-3850
Line number and SP range	CM-03 SP 10-4090
Line number and SP range	CM-03A SP 3950-6080
Line number and SP range	CM-04A SP 2710-6590

Table 5.23: *Selected acquisition parameters from Survey 77/09.*

5.5.1 CM-02

While this survey has a long recording time 12 sec in this line, penetration seems to have died out before 8 sec and anything appearing below is not considered to be real.

Processing Parameters	
Long axis / counting circle radius	10
Short axis	2
Total filled pixels	10

Table 5.24: *Key parameters used by VECSTAT in analysing CM-02.*

The results of VECSTAT's analysis of the line are presented in Table 5.25. GMT plots of the results are on CD-ROM 3:/survey77-09/CM-02/CM-02vec.pdf, CM-02eng.pdf, CM-02var.pdf.

CMP Range	Vector Mean	Circular Variance	Total Energy	Crustal Type	|r|/n	Comments
Upper	Sub-horizontal	Low	High/ focused		0.49	Undulating basement
0-7700	parallel closely			Basin	0.44	surface
lower	spaced Sub-horizontal	High	High/ focused			

Table 5.25: *The results of VECSTAT's statistical analysis of CM-02 divided into sections on the basis of crustal types. The sections used for \|r\|/n analysis are outlined on CD-ROM 3:/survey77-09/CM-02/CM-02vec.pdf and labelled a,b as in the Table.*

The profile is entirely contained within the trough and displays basin characteristics throughout. The first 2 sec TWTT is sedimentary in nature resting on an undulating basement surface. Unfortunately there is very little penetration of the actual basement with up to 1.5 sec clearly imaged. As vector means are affected by uncollapsed dipping energy at the top of the basin |r|/n readings were taken from a thin lower section of the basement. Locations are marked on CD-ROM 3:/survey77-09/CM-02/CM-02vec.pdf

5.5.2 CM-03

Like CM-02 the data quality is good down to 8 sec TWTT but again anything below is not considered to be real.

Processing Parameters	
Long axis / counting circle radius	10
Short axis	2
Total filled pixels	10

Table 5.26: *Key parameters used by VECSTAT in analysing CM-03.*

The results of VECSTAT's analysis of the line are presented in Table 5.27. GMT plots of the results are on CD-ROM 3:/survey77-09/CM-03/CM-03vec.pdf, CM-03eng.pdf, CM-03var.pdf.

CMP Range	Vector Mean	Circular Variance	Total Energy	Crustal Type	|r|/n	Comments
Upper	Sub-horizontal	Low	High/ focused		0.36[a]	
					0.386[b]	
0-8100	parallel closely spaced			Basin	0.442[c]	
	sub-	Medium	Medium/			
Lower	horizontal to sub-random		focused			

Table 5.27: *The results of VECSTAT's statistical analysis of CM-03 divided into sections on the basis of crustal types. The sections used for \|r\|/n analysis are outlined on CD-ROM 3:/survey77-09/CM-03/CM-03vec.pdf and labelled a,b,c as in the Table.*

The profile is entirely contained within the trough and displays basin characteristics throughout. Unlike CM-02 the sediment/basement interface is sub-horizontal and continuos up to CMP 7200 where it returns to more undulating from with a lot of unmigrated energy.

5.5.3 CM-03A

Again entirely contained within the Rockall Basin it data is reasonably good down to 6 sec below which everything is considered to be multiples.

Processing Parameters	
Long axis / counting circle radius	10
Short axis	2
Total filled pixels	10

Table 5.28: *Key parameters used by VECSTAT in analysing CM-03A.*

The results of VECSTAT's analysis of the line are presented in Table 5.29. GMT plots of the results are on CD-ROM 3:/survey77-09/CM-03A/CM-03Avec.pdf, CM-03Aeng.pdf, CM-03Avar.pdf.

CMP Range	Vector Mean	Circular Variance	Total Energy	Crustal Type	|r|/n	Comments
Upper 0-4200	Sub-horizontal parallel closely spaced	Low	High/ Focused	Basin	0.52[a]	Lot of unmigrated energy in basement
Lower	sub-horizontal to sub-random	Medium	Medium/ Focused			

Table 5.29: *The results of VECSTAT's statistical analysis of CM-03A divided into sections on the basis of crustal types. The section used for |r|/n analysis is outlined on CD-ROM 3:/survey77-09/CM-03A/CM-03Avec.pdf and labelled a as in the Table.*

The line continues in the same vein as rest of the survey, with sedimentary characteristics overlying those of stretched basement. There is evidence of a basement high between CMP 1200-1700 for example shows a flat sediment/basement interface elevated above the surrounding basement level. The lack of unmigrated energy in this area gives a much clearer picture of the basement below.

5.5.4 CM-04

This line continues the line into the southern part of the basin. The data quality is not as good as in previous lines and there is very poor penetration beneath the sediment/basement interface.

Processing Parameters	
Long axis / counting circle radius	10
Short axis	2
Total filled pixels	10

Table 5.30: *Key parameters used by VECSTAT in analysing CM-04.*

The results of VECSTAT's analysis of the line are presented in Table 5.31. GMT plots of the results are on CD-ROM 3:/survey77-09/CM-04/CM-04vec.pdf, CM-04eng.pdf, CM-04var.pdf.

CMP Range	Vector Mean	Circular Variance	Total Energy	Crustal Type	|r|/n	Comments
Upper 0-7800	Sub-horizontal parallel closely spaced	Low	High/ focused	Basin		Very little data in basement
lower	Sub-horizontal very little data	Low	Low		0.52	

Table 5.31: *The results of VECSTAT's statistical analysis of CM-04 divided into sections on the basis*

of crustal types. The section used for |r|/n analysis is outlined on CD-ROM 3:/survey77-09/CM-04/CM-04vec.pdf and labelled a as the results.

There is very little imaged from the basement section of this line with which to make |r|/n assessments. The depth of the sediment/water interface varies by as much as 1 sec as the line crosses what are considered to be westward spurs of the Porcupine High, at CMPs 0-1400, 3580-4800. The after 6760 the basement is at its deepest point in the survey at just over 8 sec TWTT. This marks the start of the descent into the Porcupine Abyssal Plane.

5.6 Survey 78/10

This survey was shot by Western Geophysical in October 1978, the main acquisition parameters are shown in Table 5.32. The location of the line from this survey, used in this study is shown on Figure 5.6.

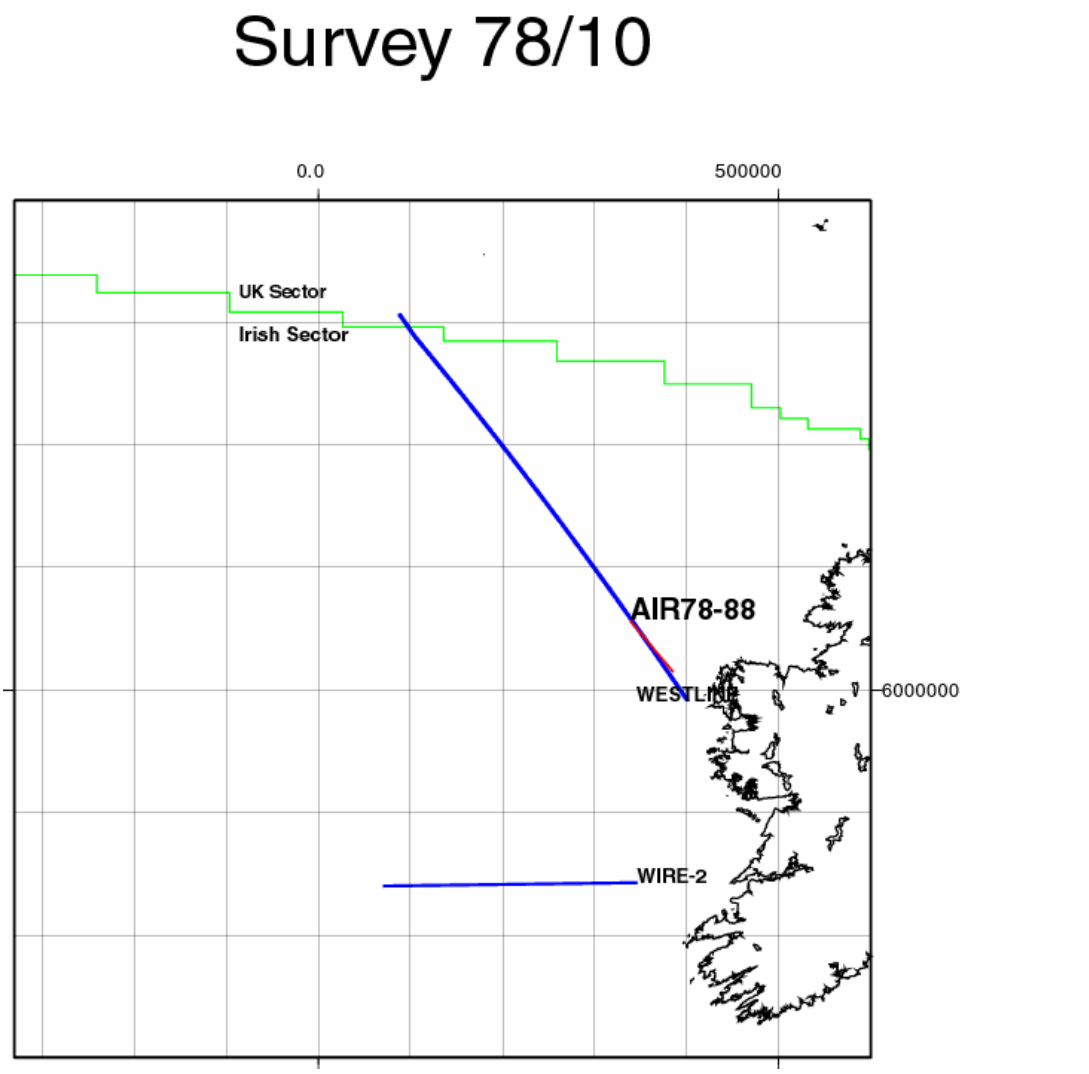

Figure 5.6: *location map showing the lines used in survey 78/10 (red), Westline and Wire-2 have been marked in blue and the boundary between the Irish and UK sectors is delineated in green.*

Survey Details	
Survey No.	78/10
Shot by	Western Geophysical
Total Survey length	1010 km
Source	Maxipulse (0.25 kg)
Source Depth	10.8 m
SP interval	200 m
Streamer length	2400 m
No of Groups	48
Group interval	50 m
Processing	DBS, 2400% stack, DAS, BPF
Vertical scale	5 cm/sec, 10 cm/sec
Horizontal scale	1:60,000 , 1:30,000
Line number and SP range	AIR78-88 SP 100-414

Table 5.31: *Selected acquisition parameters from Survey 78/10.*

5.6.1 AIR78-88

This 62.99 km line runs southeast from the Rockall Basin onto the northern part of the Slyne Basin. The quality of the data and penetration is generally good especially as the line moves onto the shelf.

Processing Parameters	
Long axis / counting circle radius	10
Short axis	2
Total filled pixels	8

Table 5.32: *Key parameters used by VECSTAT in analysing AIR78-88.*

The results of VECSTAT's analysis of the line are presented in Table 5.33. GMT plots of the results are on CD-ROM 3:/survey78-10/AIR78-88/AIR78-88vec.pdf, AIR78-88eng.pdf, AIR78-88var.pdf.

CMP Range	Vector Mean	Circular Variance	Total Energy	Crustal Type	|r|/n	Comments
0-800	Dipping	Medium-high	High	Margin		Data is noisy
800-2582	Random	High	High/ diffuse	Unst.	0.28[a]	noisy

Table 5.33: *The results of VECSTAT's statistical analysis of AIR78-88 divided into sections on the basis of crustal types. The section used for \|r\|/n analysis is outlined on CD-ROM 3:/survey78-10/AIR78-88/AIR78-88vec.pdf and labelled a as the Table.*

The data in the line was generally noisy and as a result the specific statistical characteristics are not as clear as in other lines. Two crustal types are present, margin from CMP 0-800 and unstretched basement for the rest of the line as it moves east onto the Irish shelf. There are some sedimentary layers illustrated by the parallel

closely spaced vector means at the top of the profile up to CMP 320 but the underlying basement of margin type.

5.7 Discussion

Several points of interest have arisen fro the analysis of a large collection of lines. Vector mean has emerged as the best distinguishing feature for crustal types over a range of surveys. The three patterns, random for unstretched crust, dipping in basin margin regions, and parallel closely spaced sub-horizontal layers over sub-horizontal segmented lineations in the basement for thinned stretched basement, were consistent in all surveys. That said there are slight variations but very often due to the features which are not real such as multiples or unmigrated hyperbolae, this is particularly true of margin type sections.

Total energy while consistently diffuse in unstretched basement and more focused in margin and basin settings varies a lot from survey to survey generally depending on how clean the data is. Total energy results obtained were also very sensitive to the "Total filled pixels" value chosen for the VECSTAT analysis.

Circular variance was not a very strong distinguishing feature varying greatly depending how much noise was present and how closely spaced the reflections present in the line are. Due to internal scattering in areas of focused energy areas which do not have scattered data can show high Circular variance

The results of $|r|/n$ analysis were found to be coherent within individual lines and surveys but not so across the range of surveys used. The analysis is shown to be sensitive to levels of noise within the profiles been analysed. It was also found that on the unmigrated or poorly migrated surveys that finding sufficient areas devoid of multiples or fault hyperbolae was a problem.

Conclusions

VECSTAT is capable of performing statistical analysis on data taken from any seismic data format e.g., SEGY, sgy, paper only copy. The analysis can statistically characterise the reflectivity patterns found in the seismic data and attribute to them quantities such as vector orientation.

The statistical characteristics of the reflectivity patterns have been shown to vary depending on the nature of the crust imaged. This variation can be used to map the extent of the various crustal types in the basin.

The results of vector mean analysis of strained version of an initially random data set can be used to automatically calculate the strain ratio of that data set. Taking into account the stipulations laid down in Section 4.2 this can also be applied to seismic profiles which cross basement zones which have been strained by different amounts.

Other applications include the removal of data of specified orientations for specific analysis.

Using data from the Rockall basin the applications have been tested with real data. Characterisation has been shown to work over a series of surveys with different acquisition and processing parameters with vector mean proving the most robust variable. |r|/n analysis was shown to be coherent with in particular lines and surveys but sensitive to the levels of noise within the profiles and hence results were not consistent between surveys.

Finally while this is a final annual report this is still a work in progress and maybe subject to revision or change prior to completion of a Ph.D. thesis.

References

Barton, A and White, R (1997b) Volcanism on the Rockall Continental Margin, *Geol. Soc. London*, 531-536.

Boldreel, L and Andersen, M (1993) Late Paleocene to Miocene compression in the Faeroe-Rockall Area, *Petroleum Geology of Northwest Europe: Proceedings of the fourth conference*, The Geological Society, London, 1025-1034.

Bunch, A (1979)A detailed seismic structure of the Rockall Bank (55n,15w): A synthetic seismogram analysis, *Earth Planet. Sci. Lett.*, 453-463.

Chapman, T J, Broks, R J, Corcoran, D V, Duncan, L A and Dancer, P N (1999) The structural evolution of the Erris Trough, Offshore Northwest Ireland, and implications for hydrocarbon generation, *Petroleum Geology of Northwest Europe: Proceedings of the fifth conference*, eds A J Fleet and S A R Boldy, The Geological Society, London, 445-469.

Cole, J and Peachey, J (1999) Evidence for pre-Cretaceous rifting in the Rockall Trough: an analysis using quantitative plate tectonic modelling, *Petroleum Geology of Northwest Europe: Proceedings of the fifth conference*, eds A J Fleet and S A R Boldy, The Geological Society, London 359-370.

Corfield, S, Murphy, N and Parker, S (1999) The structural and stratigraphic framework of the Irish Rockall Trough, *Petroleum Geology of Northwest Europe: Proceedings of the fifth conference*, eds A J Fleet and S A R Boldy, The Geological Society, London, 407-420.

Croker, P and Shannon, P (1987) The evolution of the hydrocarbon prospectivity of the Porcupine Basin, offshore Ireland, *Petroleum Geology of North West Europe*, Graham and Trotman (eds) ,633-642.

Daly, J, Heaman, L, Fitzgerald, R, Menuge, J, Brewer, T, and Morton, A (1995) Geochronological and Isotopic constraints on the age and crustal evolution of the crystalline basement in Western Ireland and Rockall, *Petroleum Geology Ireland's offshore Basins*, The Geological Society, London, **93**, 433-434.

Einsele, G (1985) Basaltic sill-sediment complexes in young spreading centres: genesis and significance, *Geology*, **13**, 249-252.

England, R and Hobbs, R (1997) The structure of the Rockall Trough imaged by deep seismic reflection profiling, *J. Geol. Soc. London*, **154**, 497-502.

Goldman M (1999) SEGY to ASCII conversion and Plotting Program, http://geology.wr.usgs.gov/open-file/of99-126

GMT (2001) GMT - The Generic Mapping Tools Version 3.4, http://gmt.soest.hawaii.edu/

Haszeldine, R S (1984) Carboniferous North Atlantic palaeogeography: stratigraphic evidence for rifting, not megashear of subduction, *Geology Magazine*, **121**, 443-463.

Hauser, F, O'Reilly, B, Jacob, B, Shannon, P, Makris, J, and Vogt, U (1995) The crustal structure of the Rockall Trough: Differential stretching without underplating, *J. Geophys. Res.*, **100**(B3), 4097-4116.

Hewlard Packard (1997) *The Hp-GI/2 and Hp Rtl Reference Guide: A Handbook for program developere,* 3rd edition, Addison-Wesley, 516p.

Joppen, M and White, R (1990) The structure and subsidence of Rockall Trough from two-ship seismic experiments, *J. Geophys. Res.*, **95**(B12), 19821-19837.

Knott, S D, Burchell, M T, Jolley, E J and Fraser, A J (1993) Mesozoic to Cenozoic plate reconstructions of the North Atlantic and hydrocarbon plays of the Atlantic margins, *Petroleum Geology of Northwest Europe: Proceedings of the fourth conference*, ed R J Parker, The Geological Society, London, 953-974.

Le Hors (2001) The XPM Format and Library, http://koala.ilog.fr/lehors/xpm.html

Makris, J, Ginzburg, A and Shannon, P (1991) A new look at the Rockall region, Offshore Ireland, *Marine and Petroleum Geology*, **8**, 410-416.

Masson, D and Miles, P (1986) Structural development of the Porcupine Seabight sedimentary basin, offshore Southwest Ireland, *Am. Ass. of Petrol. Geol. Bull.*, **70**, 567-548.

Musgrove, F W and Mitchener, B (1996) Analysis of pre-Tertiary rifting history of the Rockall Trough, *Petroleum Geoscience*, **2**, 353-360.

Nadin, P A, Houchen, M A and Kusznir, N J (1999) Evidence for pre-Cretaceous rifting in the Rockall Trough: an analysis using quantitative 2D structural/stratigraphic modelling, *Petroleum Geology of Northwest Europe: Proceedings of the fifth conference*, eds A J Fleet and S A R Boldy, The Geological Society, London, 371-378.

Naylor, D, Shannon, P and Murphy, N (1999) *Irish Rockall Region – a standard nomenclature system*, Petroleum Affairs Division, Special Publication 1/99, 42pp.

O'Reilly, B, Hauser, F, Jacob, B, and Shannon, P (1996) The lithosphere below the Rockall Trough: wide-angle seismic evidence for extensive serpentinisation, *Tectonophysics*, **255**, 1-23.

Roberts, D G and Jones, M T (1978) A bathymetric, magnetic and gravity survey of the Rockall Bank, H.M.S. Hecla 1969, Admiralty Marine Science Publication, **19**, 45pp.

Sanderson D J (1977) The analysis of finite strain using lines with initial random orientation, *Tectonophysics*, **43**, 199-211.

Shannon, P (1991) The development of Irish Offshore sedimentary basins, *J. Geol. Soc. London*, **148**, 181-189.

Shannon, P, Jacob, B, Makris, J, O'Reilly, B, Hauser, F, and Vogt, U (1995) Basin development and petroleum prospectivity of the Rockall and Hatton Region, *The Petroleum Geology of Ireland's offshore basins*, The Geological Society, London, **93** 435-447.

Ryan, J. L., Lonergan, L., and Jolly, R. (2000) Fractal spacing and orientation distribution for 2D datasets, *J. Geophy. Res.*, 105(D8), 19,505-19,320.

Vogt, U, Makris, J, O'Reilly, B, Readman, P, Jocob, B, and Shannon, P (1998).The Hatton Basin and continental margin: Crustal structure from wide angle seismic and gravity data, *J. Geophys. Res.*, **103**(B6), 12545-12566.